COPY

GL-TR-90-0173

AD-A227 966

A Study of the Interaction of Physical and Numerical Parameterizations With Regard to Moisture Forecasting in a Regional Model of the Atmosphere

Isidore M. Halberstam
S-L. Tung
L. Knowlton
G. Zolotusky

ST Systems Corporation
109 Massachusetts Avenue
Lexington, MA 02173

25 July 1990

Final Report
May 1988 - May 1990

Approved for public release; distribution unlimited

Geophysics Laboratory
Air Force Systems Command
United States Air Force
Hanscom Air Force Base, Massachusetts 01731-5000

This technical report has been reviewed and is approved for publication.

CHIEN-HSIUNG YANG
Contract Manager

DONALD A. CHISHOLM
Atmospheric Prediction Branch

FOR THE COMMANDER

ROBERT A. McCLATCHEY, Director
Atmospheric Sciences Division

REPORT DOCUMENTATION PAGE

Form Approved
OMB No. 0704-0188

1. AGENCY USE ONLY *(Leave blank)*

2. REPORT DATE
25 July 1990

3. REPORT TYPE AND DATES COVERED
Final Report (May 1988–May 1990)

4. TITLE AND SUBTITLE
A Study of the Interaction of Physical and Numerical Parameterizations With Regard to Moisture Forecasting in a Regional Model of the Atmosphere

5. FUNDING NUMBERS
PE 61102F
PR 2310 TA G7 WU DD
Contract F19628-88-C-0072

6. AUTHOR(S)
Isadore M. Halberstam
S-L. Tung
L. Knowlton
G. Zolotusky

7. PERFORMING ORGANIZATION NAME(S) AND ADDRESS(ES)
ST Systems Corporation
109 Massachusetts Avenue
Lexington, MA 02173

8. PERFORMING ORGANIZATION REPORT NUMBER

9. SPONSORING/MONITORING AGENCY NAME(S) AND ADDRESS(ES)
Geophysics Laboratory
Hanscom AFB, MA 01731-5000

Contract Manager: C. H. Yang/LYP

10. SPONSORING/MONITORING AGENCY REPORT NUMBER
GL-TR-90-0173

11. SUPPLEMENTARY NOTES

12a. DISTRIBUTION/AVAILABILITY STATEMENT
APPROVED FOR PUBLIC RELEASE; DISTRIBUTION UNLIMITED

12b. DISTRIBUTION CODE

13. ABSTRACT *(Maximum 200 words)*
This is the final report produced under contract F19628-88-C-0072. It summarizes the research performed with STX's Relocatable Limited-Area Model (RLAM) in assessing the necessary ingredients for forecasting moisture. The report describes the experiments involving lateral boundary treatment and physical parameterizations of the planetary boundary layer (PBL) and convective systems. It also explains how these interact with the numerical schemes that are available in RLAM and what effects these have on moisture forecasts.

14. SUBJECT TERMS
Regional modeling
Numerical weather prediction
Finite-difference methods
Convective parameterizations
Boundary conditions
Planetary boundary layer
Atmospheric modeling

15. NUMBER OF PAGES
66

16. PRICE CODE

17. SECURITY CLASSIFICATION OF REPORT	18. SECURITY CLASSIFICATION OF THIS PAGE	19. SECURITY CLASSIFICATION OF ABSTRACT	20. LIMITATION OF ABSTRACT
Unclassified	Unclassified	Unclassified	SAR

ACKNOWLEDGMENTS

The authors express their gratitude to Dr. C-H Yang for his guidance and constant assistance in directing this research. They also appreciate the technical assistance provided by Mr. Donald Norquist and the superb manuscript preparation of Ms. Norma Tocco.

TABLE OF CONTENTS

LIST OF FIGURES

LIST OF FIGURES (continued)

LIST OF TABLES

I. Introduction

The Relocatable Limited-Area Model (RLAM) of ST Systems Inc. has been described extensively in Gerlach (1988, 1986, and 1985) and Tung, et al. (1987). RLAM, because of its many attributes, allows for studying the effect of various combinations of physical and numerical parameterizations. Under terms of the present contract, STX combined and tested selections of convective and boundary layer parameterizations, fourth- and second-order spatial differencing, high and low horizontal resolution, radiation and sponge lateral boundaries, and Lagrangian and Eulerian advections of moisture. These tests sought to determine crucial parameters needed for the accurate prediction of moisture by inclusion of different parameters in several forecast experiments over independent scenarios.

The next section will describe RLAM and the various schemes available. The third section will describe the experiments performed and their results. The fourth section will present our conclusions and the final section will contain our recommendations based on these experiments.

II. RLAM and Its Selections

A full description of RLAM can be found in the works cited in the previous section. A short summary of pertinent selections will be mentioned here along with more detailed descriptions of newly implemented processes. RLAM is a mesoscale model with variable horizontal and vertical resolution and specifiable domain size and location. Coordinate systems are $\sigma = p/p_s$, where p is pressure and p_s is surface pressure, in the vertical and Cartesian map coordinates in the horizontal. The map projection may be conformal, i.e., mercator, lambert, or polar, or spherical coordinates may be selected. The equations are written in generalized form with the map factors compensating for differences in projection. Obviously, map projections cannot be chosen with impunity; mercator projections at the pole or lambert projections at the equator will not work and it is necessary for the user to choose a projection best suited to the region of interest.

Numerical differencing can be performed by either second- or fourth-order. Fourth-order differencing requires more lateral boundary points than second-order, but results in theoretically smaller truncation error. Fourth-order compact differencing allows for less boundary points but requires assumptions about the derivative at the boundary, which effectively cancel any presumed benefit of the scheme. Hence, fourth-order compact differencing is no longer a choice for RLAM. Vertical and horizontal resolution are set by choosing for the grid configuration, respectively, the σ-coordinates and a fraction of the standard mesh size, equal to one bedian (about 400 km). The number of grid points selected will then determine the size of the domain.

The temporal scheme can be a regular leap-frog or a modified leap-frog with time-averaged pressure gradients as described by

Brown and Campana (1978). Both of these are subject to CFL restrictions on the time step, even the Brown-Campana scheme, hence a semi-implicit scheme was introduced based on the model of the Bureau of Meteorology Research Centre (BMRC) of Australia (see McGregor et al., 1978). The scheme, however, was not easily adaptable to RLAM (Halberstam, 1989) because the matrix that related surface pressure tendency to the temperature tendency tempered by non-linear terms was essentially ill-conditioned and created large discrepancies in the surface pressure forecast when minor modifications were enacted in the model. We, therefore, did not retain the semi-implicit scheme as an alternative and all experiments discussed here were performed with the Brown-Campana scheme.

A new implicit filter was also added to the model in parallel with the Shapiro (1970) filters. It was created by Raymond (1988), and has the advantage of being very selective as to which wavelengths are removed. The filter is invoked at every time-step and the degree of smoothing is controlled by setting its parameters. In most of the experiments, the Raymond filter showed very little difference from the Shapiro filter.

Initial conditions were derived from FGGE IIIB in one of two ways. Originally, the spectral field prepared for the Air Force Geophysics Laboratory's (GL) global spectral model (GSM) was expanded at the desired grid points of RLAM and used as the initial field for the RLAM forecast. The more recent method involves a direct bilinear interpolation from FGGE IIIB data to the desired grid. The field is then interpolated vertically to the desired σ layers from the FGGE mandatory levels. There are some significant differences in resulting forecasts depending upon which initial field is used, despite the fact that FGGE IIIB data have been initialized, mainly because there is a different level of smoothing and hence an essentially different initial field created by each method.

Other innovations made to RLAM need to be described in greater detail:

A. Lagrangian Advection of Moisture

In keeping with Ritchie's (1985) suggestion that moisture be advected by quasi-Lagrangian rather than Eulerian representation, we investigated the effects such an advection scheme would have on the moisture distribution and precipitation. RLAM solves its set of equations (see Gerlach, 1988, Eqs. 1) by calculating all terms on the right-hand side, i.e., all terms which affect the tendency of the dependent variables. Physical processes including convection and boundary layer exchanges also appear as terms which affect the tendency of the variables. With the explicit time schemes, the variables are all updated in unison, given their tendencies based on values from the current and previous time steps. Moisture, as one of the dependent variables, is handled in the same manner. For the sake of Lagrangian advection, it seemed advantageous to separate moisture from the other variables and treat it after all other variables have already been forecast. But that also implied that the calculations of moisture physics which depended on values of moisture would also have to be postponed until after moisture had been forecast. Thus, all subroutines dealing with physics were called only after an interim forecast value of all variables had already been obtained based on the advective and adiabatic portions of the equations. Diagram 1 shows the flowchart for each of these methods, with the customary convention for representing variables: u, v are wind velocity components, T is temperature, q is specific humidity, and p_s is surface pressure, while the superscript n signifies time step. The main difference between the two algorithms is that the first deals with physics as an integral part of the model tendencies, whereas the second sees physics as an after-the-fact adjustment to the predicted variables.

The Lagrangian advection itself is accomplished by first advecting moisture from the grid point and then interpolating back from the advected locations to the grid points. At first, we attempted to advect the moisture parcel in two dimensions using both velocity components and then interpolate back to the grid points with a bi-cubic spline supplied by IMSL software. Unfortunately, the bi-cubic spline is a very slow procedure and greatly increased the execution time of the model. We, therefore, heeded a suggestion by Jiamo (1988) and separated the advection into three distinct one-dimensional processes. First, we advected the parcel while conserving the moisture in the x direction given

DIAGRAM 1 - Flowcharts for the forecasting
of variables in RLAM

1. Original with Eulerain advection

Compute tendencies
for u, v, T, q, and ln p_s

Calculate physical processes

Invoke time scheme to obtain
u^{n+1}, v^{n+1}, T^{n+1}, q^{n+1}, and ln ${p_s}^{n+1}$

DIAGRAM 1 - Flowcharts for the forecasting of variables in RLAM (continued)

2. Revised with Lagrangian or Eulerian advection. For Lagrangian advection, q (in parentheses) is omitted. For Eulerian advection, third box is omitted.

Compute tendencies for
u, v, T, (q), and p_s

without physical processes

Invoke time scheme to produce interim values of

u^{n+1}, v^{n+1}, T^{n+1}, (q^{n+1}), and $\ln {p_s}^{n+1}$

If Lagrangian, combine

u^{n+1}, v^{n+1}, with u^n, v^n to

obtain interim q^{n+1}

Calculate physical changes based on interim values and update variables to obtain final version of

u^{n+1}, v^{n+1}, T^{n+1}, q^{n+1}, and $\ln {p_s}^{n+1}$

the value of u^n at the grid points. After locating the parcel on the x-axis, a linear interpolation was performed to determine u^{n+1} at that location. A new velocity component u, equal to the average of u^n at the grid point and the interpolated u^{n+1}, was used to again advect the parcel from the grid point to a new location on the x-axis. (This averaging and advecting could have been iterated to obtain a higher degree of refinement; however, as with most quasi-Lagrangian models, such a process would have become impractical.) Given the new locations on the x-axis and the lateral boundary values of q from the GSM, a one-dimensional cubic spline was employed to interpolate back to the grid points. The whole process was then repeated for these newly derived moisture values in the y direction using the v component of velocity. The process was then repeated a third time in the vertical using the vertical velocity σ. The IMSL package available to us offered three routines for cubic spline iterpolation. We tested each one and found very little difference in results. We therefore selected the simplest version known as CSINT but retained the option of calling any of the others. We also tested this separated advection approach to determine whether order played a significant role in the outcome. We found that when we advected in the y direction first and in the x direction second, results differed from the first ordering by only .1%. Advection in the vertical was very similar to the horizontal, except that there are no "boundary conditions" to anchor the values at either end. If all advected air parcels are above the bottom σ-layer and/or below the top

σ-layer, the cubic spline extrapolates a value based on the closest set of data points.

B. Lateral Boundary Treatment

In previous reports (Gerlach 1986 and 1988), we described the handling of RLAM's lateral boundary by means of a relaxed Davies (1976) or Perkey-Kreitzberg (1976) boundary. These boundary treatments are based on the concept of a transition zone between the externally specified values and the internally specified values generated by the regional model. The externally specified values are inserted fully at the outermost row. Some rows in, only the model-generated values can be found. Between these two extremes, the external and internal values are combined using weights to favor either the external or internal values. Davies (1976) deals with the variables themselves and relaxes the boundary region by adding a weighted Laplacian of the differences between the internal and external fields. Perkey and Kreitzberg (1976) deal with the computed tendencies and use weights to determine the final tendencies. Smoothing is performed at the boundaries after the forecast values are derived to prevent high-frequency waves from entering the region. A drawback of these methods is that they require saving several rows of boundary data from an external source.

Another class of boundary treatments was added to RLAM, modeled after Orlanski's (1976) radiation boundary. Here, the velocity of propagation of a variable is calculated near the boundary. If the direction of propagation is away from the boundary, the wave is allowed to exit by advecting the internal values to the boundary with its speed of propagation. If the direction of propagation is inwards, however, the externally provided values are inserted at the outermost boundary row. A refinement to the Orlanski calculation of phase velocities was made by Miller and Thorpe (1981). We added this as an option and found that it did improve performance of the radiation boundary. Another suggestion by Carpenter (1982) to include the external values in the calculation of the phase velocities was also added to the model, but we found that this innovation frequently caused the model to become unstable. Seitter (1987) also proposed some variations on Orlanski's theme. One was that the velocities of all mass and momentum variables (i.e., T, u, v, and p_s) be determined and their average used to advect all of them. We added that option to the lateral boundary repertoire, as well. We also introduced a new boundary treatment that merges features of Lagrangian schemes with the radiation boundary. Values near the boundaries were advected by the wind velocities, not phase velocities, in a conservative manner to locations away from the grid points. These advected quantities could then serve as new data points at the forecast time. The boundary values could then be estimated by a crude analysis involving the external values, the updated internal values, and the advected values. Various weights could be given to these data points depending on source (external or internal) and distance from the desired boundary point. One could also decide how many points should be included in the interpolation-extrapolation. We also allowed the option, as with the radiation scheme, to turn off the interpolation and simply insert the external values, if the propagation velocity were directed inward.

C. Physical Parameterizations

RLAM's physical parameterizations had consisted of a bulk parameterization of the planetary boundary layer (PBL), a large-scale precipitation scheme, and a Kuo (1974) cumulus convective scheme. These had been adapted from Mathur's (1983) quasi-Lagrangian nested grid model (QMGM), which, in turn, had adapted them from NMC's spectral model, (Sela, 1980). These parameterizations were also basically the same as those applied to the GSM at the beginning of its development. Recently, these older parameterizations were replaced by newer, and hopefully better ones, developed by the University of Illinois (Soong, et al., 1985) and Oregon State University (OSU) (Mahrt, et al., 1987). These are still being studied by GL and some modifications to the original package are still being made. It is these latest convective and PBL schemes of the GSM that we adapted to RLAM during the course of this research.

Soong, et al., (1985) present a cumulus convection scheme that is similar in construct to Kuo's (1974) original formulation but one which incorporates several new features. Among these are the explicit calculation of the parameter b, which is the fraction of moisture applied to atmospheric moistening as opposed to precipitation, the inclusion of entrainment, and the estimation of the height of the cloud from weak to strong convection. The entrainment process, although seemingly accurate in forecasting convective processes in GATE, presented many problems in the estimation of global-scale precipitation. Indeed the inclusion of entrainment tended to decrease precipitation unrealistically and moisten the normally dry upper atmosphere. For this reason it was removed from the convective scheme of the GSM and, after several tests on RLAM showing the same results, removed from RLAM as well. In addition, the GL GSM modelers assumed that only part of the grid box should be subject to condensation or evaporation, and imposed a fraction that represented the portion of the grid box covered by cloud.

Mahrt, et al., (1987) present a PBL model which is radically different from the bulk parameterization previously employed by the GSM. The new OSU PBL expends a great deal of effort in calculating the soil-atmosphere exchange of heat and moisture by specifying such factors as soil type, vegetative cover, and soil moisture. It also parameterizes the surface layer turbulence fluxes and attempts to smooth out the normally sharp transitions between stable and unstable fluxes. The variable flux layer above the surface layer is also modeled, and the height of the PBL is a predicted quantity. The model requires higher resolution in the lower layers of the atmosphere, more than is available with the 17 σ-layer configuration adopted in previous RLAM experiments. Instead, an

18-layer model is substituted with increased resolution in the lowest levels. The model also requires a radiation balance at the surface, a capability that RLAM does not possess. OSU, however, does provide a "poorman's version" of a radiation scheme based only on the sun's declination and time of day. The radiation scheme then produces a crude estimate of the incoming short-wave and outgoing long-wave radiation. This scheme was adapted to RLAM rather easily. The two new schemes, PBL and convective, were tested both independently and in combination with each other.

III. Results

In discussing results, we are relying on experiments for three independent scenarios. The first is the famed Presidents' Day storm off the East Coast of the U.S. on 18-19 February 1979. As mentioned in earlier reports (Gerlach, 1985), this case is particularly suited for study by limited-area models because of its rapid development apparently from sub-grid size phenomena. We have already shown the importance of physical parameterization in forecasting the storm and the introduction of new physical packages in RLAM made a re-examination of this case a logical step. The second case was an occluded system that brought a great deal of precipitation to the East Coast between 23 and 25 January of the same year. The third event was a summertime depression over the North Sea that moved rather slowly during 24 to 26 June 1979. The latter two events were easier to forecast by dint of their being older, more developed systems that did not undergo rapid changes and may, therefore, serve as benchmarks for the GSM and the various runs of RLAM each with its own particular combination of parameters.

As a point of reference, we present the synoptic situation as depicted by FGGE IIIB analyses at 1200 UTC 26 June 1979 over northern Europe, at 1200 UTC 19 February 1979 over North America, and at 0000 UTC 25 January 1979, in Figs. 1, 2, and 3, respectively. In Figs. 1 and 3, the prominent storm systems are nearly occluded and have a history of many hours, if not days. The situation in Fig. 2 is quite different, where a sudden deepening of the surface system in conjunction with an upper air trough gave rise to the severe snowstorm depicted by the low pressure on the East Coast. The storm has been well documented in the literature as discussed in our earlier reports (Gerlach, 1985). Suffice to say, it was a very difficult storm to forecast and most operational models of the time completely missed its development.

A. Lateral Boundary Experiments

The various forms of handling the lateral boundaries produced significantly different results. The Davies boundary produced the smoothest transition at the boundary and, in combination with a Shapiro or implicit filter, was able to suppress most unwanted high-frequency waves. Fig. 4a is an example of a Davies boundary 48 h RLAM forecast of sea-level pressure at 1200 UTC 26 June over Europe and the North Sea. In general, the forecast seems rather

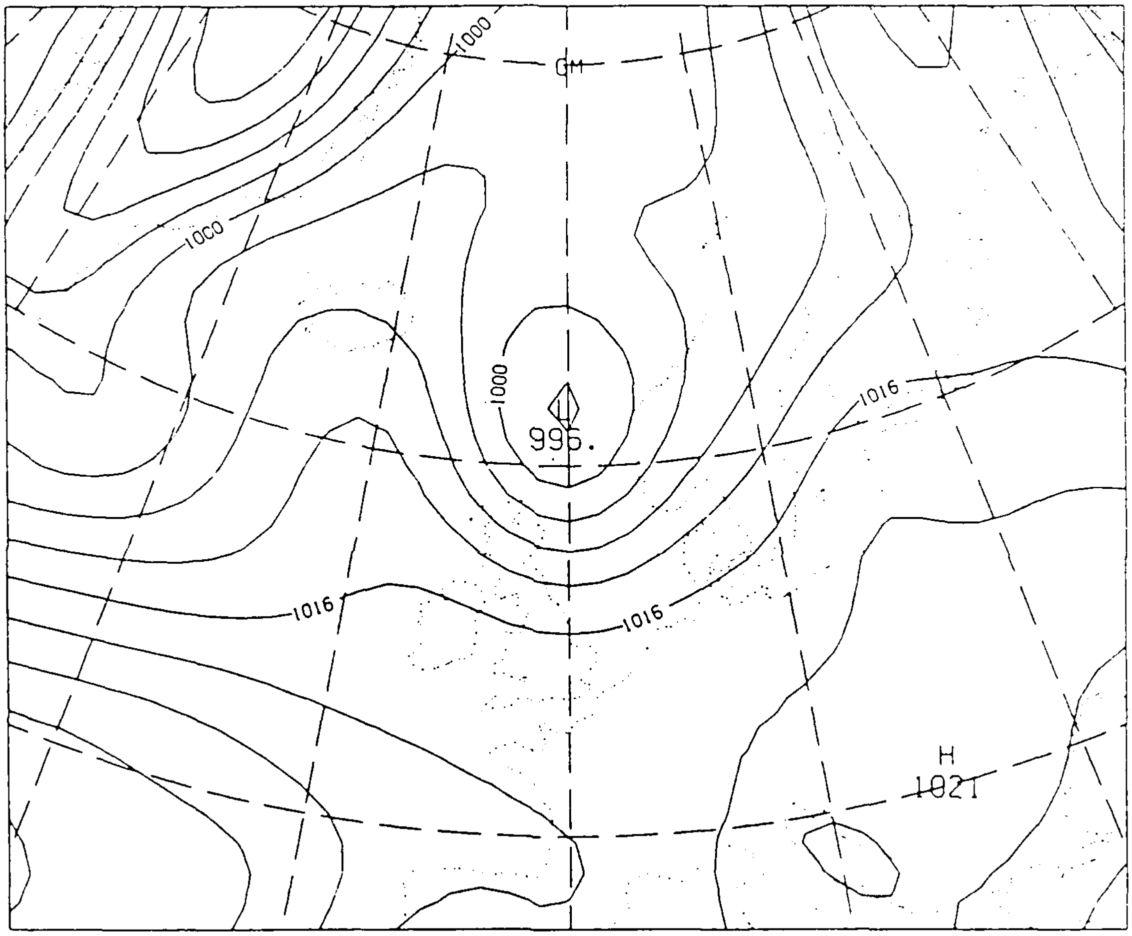

Figure 1

FGGE IIIB analysis of sea-level pressure at 1200 UTC 26 June 1979 for the North Sea and environs. Contours are marked in mb.

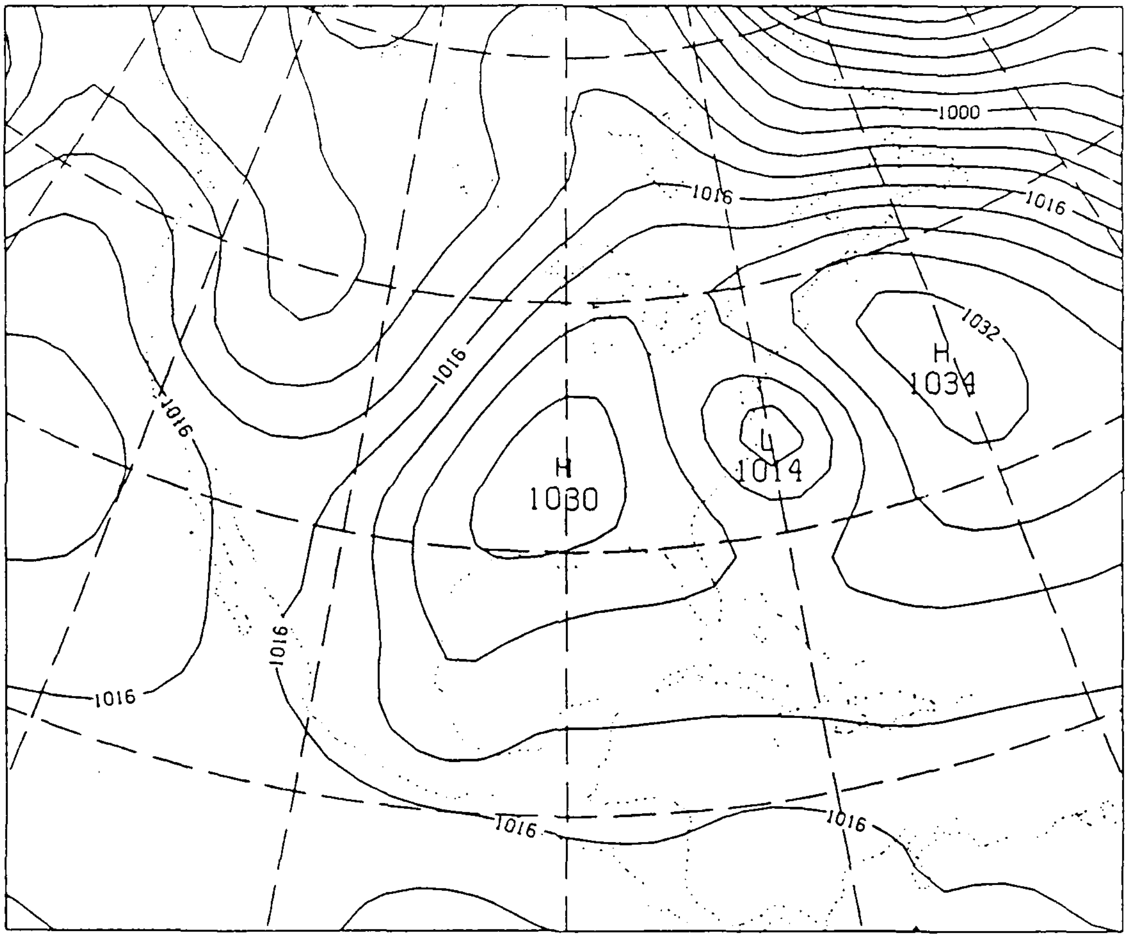

Figure 2

Same as Fig. 1, except for 1200 UTC 19 February 1979 over North America.

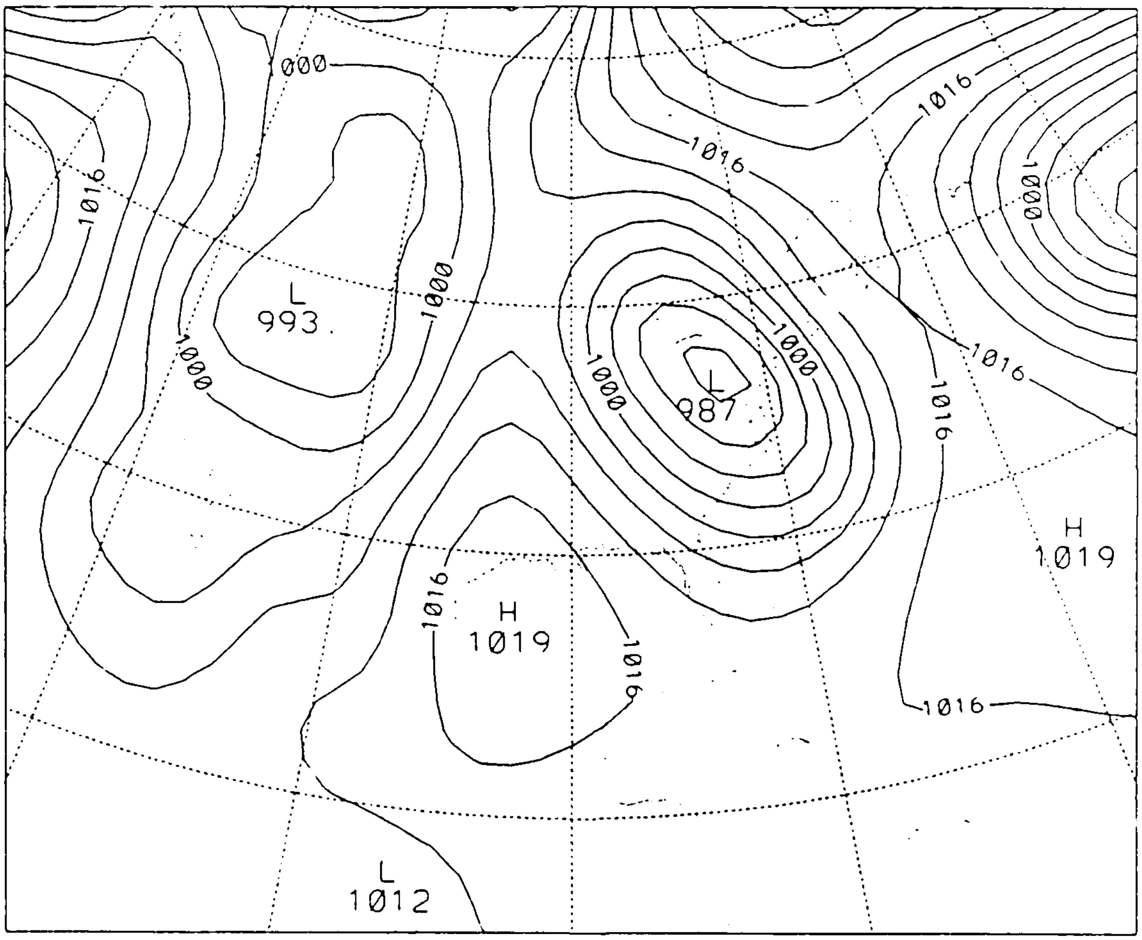

Figure 3

Same as Fig. 1, except for 0000 UTC 25 January 1979.

good, with only a slight overdeepening of the surface low west of Norway and over Greenland. Fig. 4b depicts a 48 h forecast with Orlanski's boundary (with the Miller and Thorpe, 1981, modification). The interior of the field is much the same as the Davies forecast, but there is a noticeable deterioration at the boundaries. Some spatial noise is quite apparent on some of the contours, especially at the boundaries. Fig. 4c is the 48 h forecast with the phase speed averaged over all variables as suggested by Seitter (1987). Here again, the interior is affected only little, but the boundaries are quite noisy, even more than for Orlanski's treatment. In contrast, Fig. 4d is the GSM 48 h forecast for the same region, made with 17 layers and 30 rhomboidal waves. This forecast is strikingly similar to the RLAM forecast with the Davies boundary, despite the differences in algorithms and numerical parameterizations between the two models.

The Lagrangian boundary that we developed did not fare much better than the radiation boundaries. There is some flexibility in the choice of weights and radius of influence and several combinations were tested. In general, the weights were determined by first giving the large-scale, external variable an arbitrary weight, F_{LS}, normally about 1.0. The weights of other points near the boundary are determined by

$$F_n = 1 - [(\delta x_n/k\,\Delta x)^2 + (\delta y_n/k\,\Delta y)^2], \qquad (1)$$

where δx_n, δy_n are the distance components from the boundary point

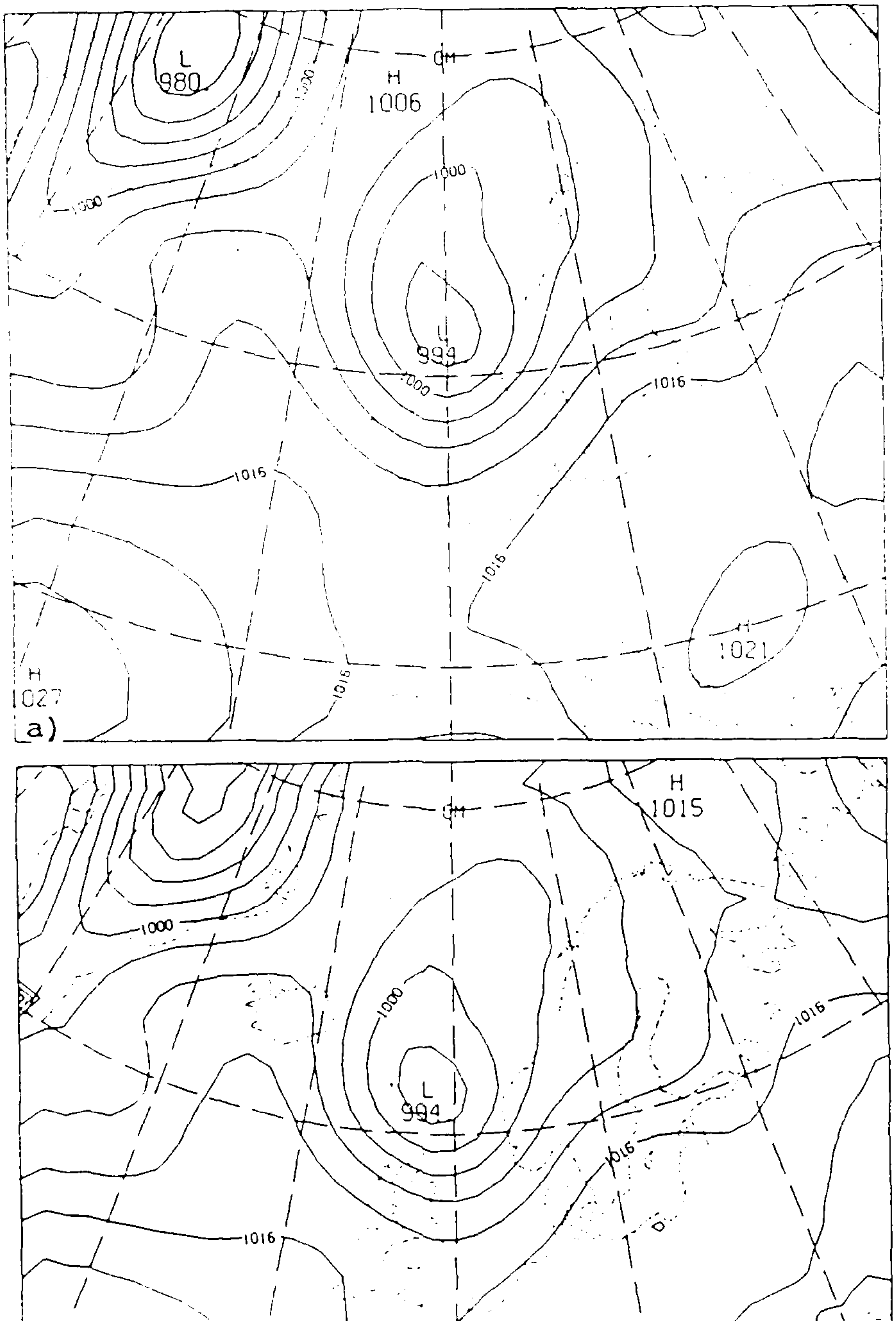

Figure 4

48 h forecast of sea-level pressure valid at 1200 UTC 26 June 1979 over the North Sea by RLAM with a) Davies boundary treatment, b) Orlanski radiation boundary, and c) averaged phase velocity radiation boundary, and d) GSM with 17 layers and 30 rhomboidal waves.

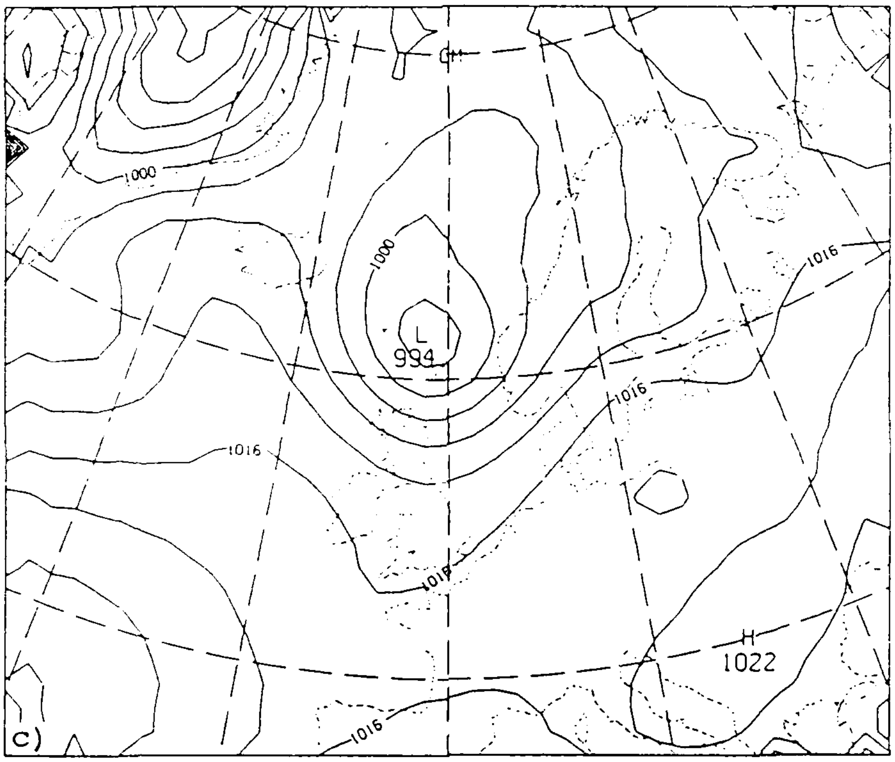
1000
1000
L
994
1016
1016
1016
1016
H
1022
1016
c)

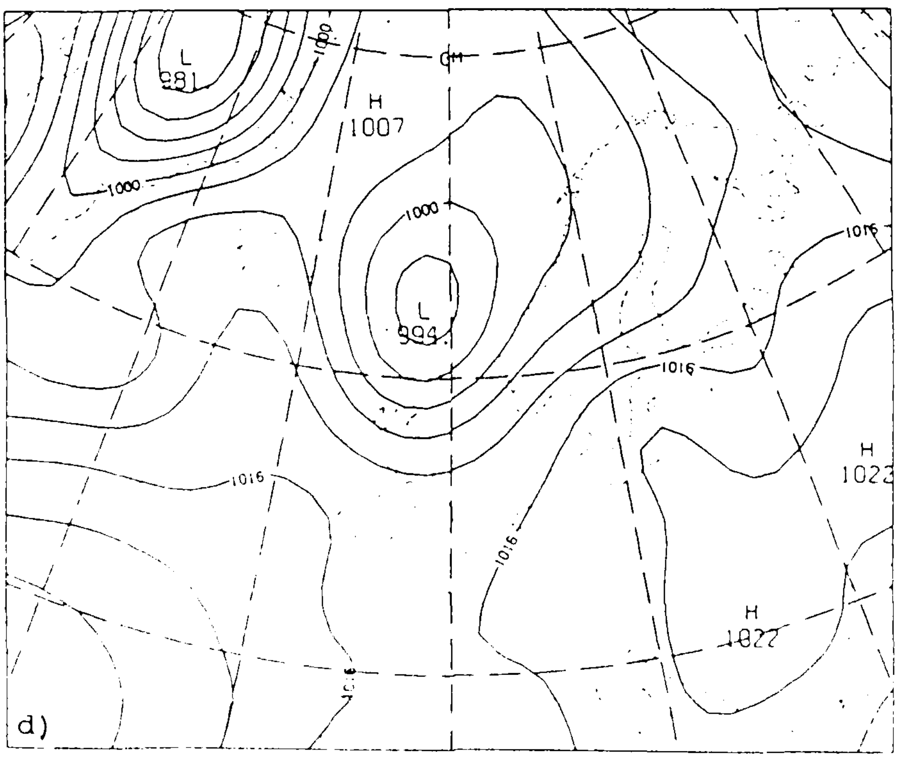
L
981
1000
H
1007
1000
1000
L
994
1016
1016
1016
H
1022
1016
H
1022
d)

that the advected entities from neighboring grid points lie. The parameter k determines how far we wish to extend the radius of influence and how many points should be part of the interpolation. If k = 1, then no other grid point will influence the boundary but advected points will have an influence if they are advected from the interior towards the boundary. If they are advected away from the boundary, the boundary point will automatically receive the value of the large scale. The final weights are determined by adding the values determined by (1) to the value assigned to the large scale, F_{LS}, and dividing each F_n by the sum to normalize the weights. The value at the boundary is determined by adding the product of the weights and the individual values, namely

$$Q_b = W_{LS}\ Q_{LS} + \sum_{j=1}^{N_k} W_j\ Q_j,$$

where Q is any variable and the W's are the normalized weights. N_k is the number of points involved in the interpolation to each boundary point, and is dependent on k.

Fig. 5a is the forecast based on Lagrangian boundaries with F_{LS} = 1.0 and k = 1. Fig. 5b portrays the 48 h forecast for a Lagrangian boundary with k = 2, F_{LS} = 1.0, while Fig. 5c sets k = 2, F_{LS} = 1.2 and increases the smoothing interval from every third time step at the boundaries and every ninth time step in the interior to every time step at the boundaries and every third time

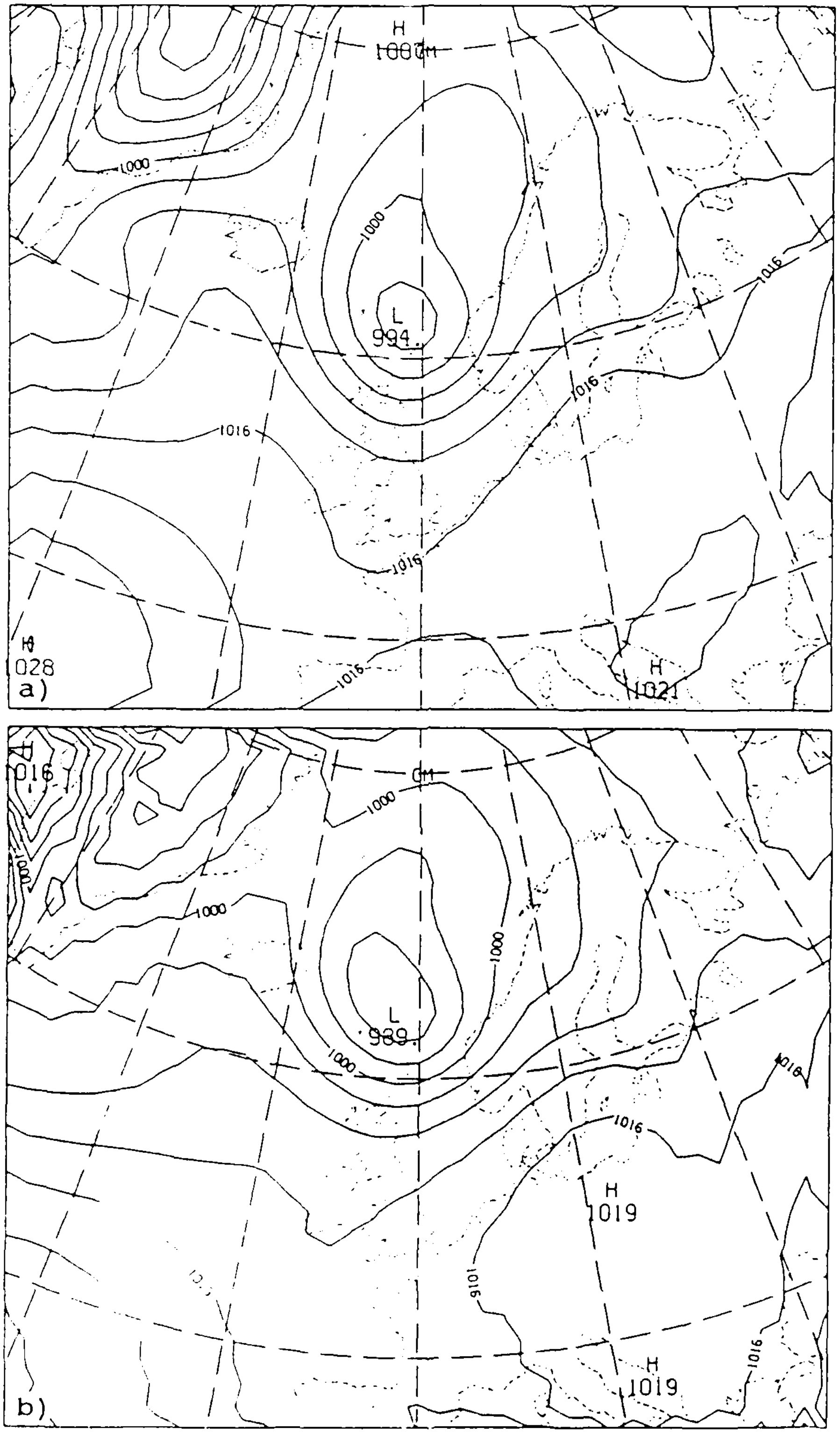

Figure 5

Same as Fig. 4, except for Lagrangian boundary treatment with a) F_{LS} = 1.0, k = 1, smoothing every third time step at boundary and every ninth time step in interior (3,9), b) F_{LS} = 1.0, k = 2, smoothing at 3,9, and c) F_{LS} = 1.2, k = 2, and smoothing at 1,3.

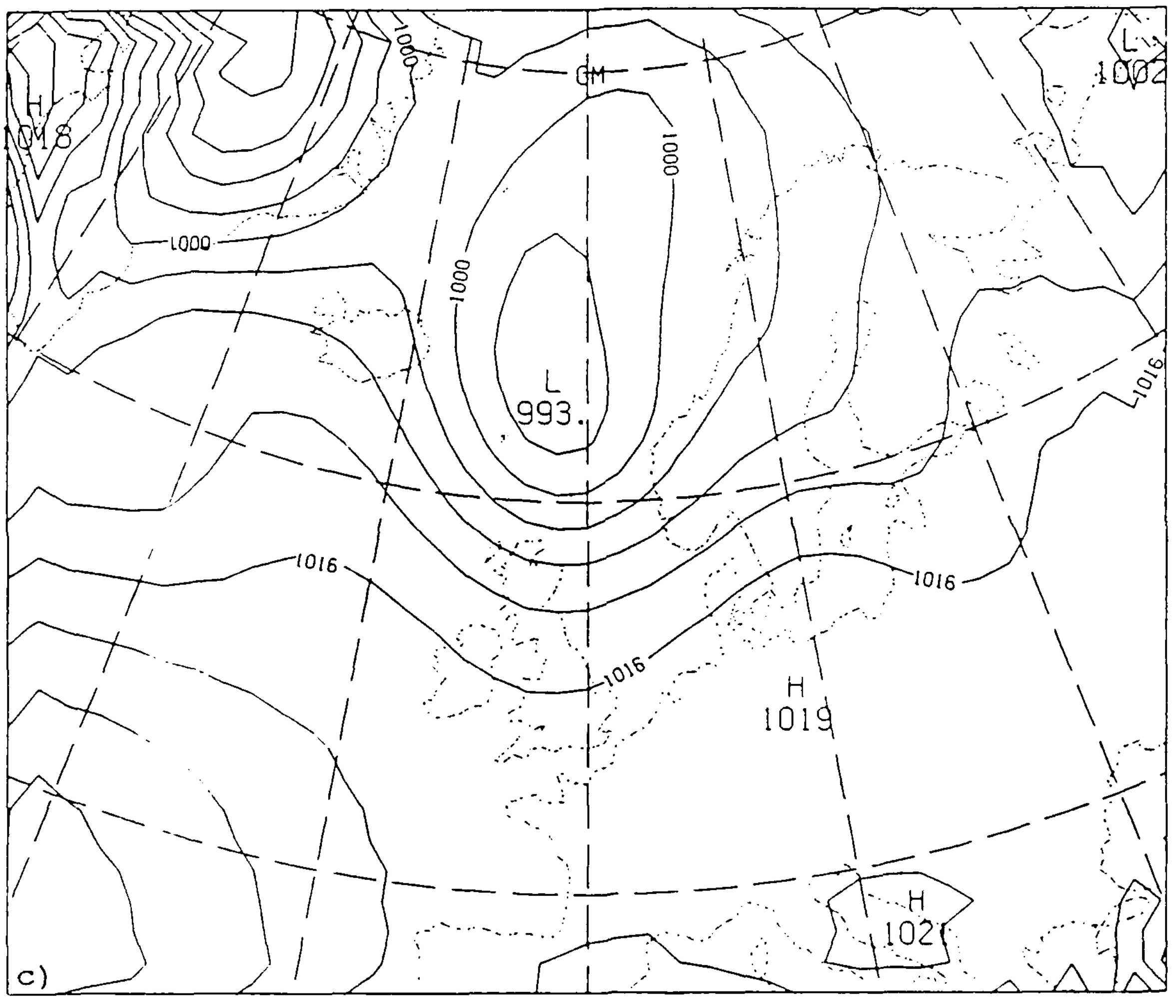
H
1018
1000
GM
L
1002
1000
1000
1000
L
993.
1016
1016
1016
1016
H
1019
H
102
c)

step in the interior. The latter two show clearly that the Lagrangian boundary fares no better than the radiation boundary. Even with increased smoothing the northwest corner over Greenland is extremely noisy. Much of that noise is visible even in the interior of the field, which is apparently reacting to the poor boundary specification and is noticeable in the central pressure of the low near Great Britain. Fig. 5a seems a bit more promising since it resembles very closely the Davies boundary forecast of Fig. 4a. But this optimism is not warranted because the Lagrangian boundary portrayed in 5a is identical to a forecast produced with nothing more than the insertion of the large-scale intact at the outermost row. Apparently, in the case of low weight and small radius the Lagrangian advection, especially, because of the small time step involved ($\Delta t = 120$ s), has no effect on the boundaries.

These results were essentially replicated for the other two scenarios, supporting Seitter's (1987) contention that the radiation boundaries, while theoretically alluring, still leave a lot to be desired. Among many other problems is the ageostrophic imbalances which cause frequent switching of the direction of the phase velocity which, in turn, controls whether internal or external values are inserted at the boundaries. By averaging the velocities for the mass and momentum variables, the problem is magnified when the direction of the velocity for one variable implies external values, while another variable requires extrapolated internal values. The Lagrangian boundaries also give rise to spurious waves at the boundaries whenever other than the large scale is involved. When only the large scale is inserted, forecasts may succeed as in the example presented here, but they may easily fail. Whether some combination of weights and smoothing may be found to make the Lagrangian boundary useful remains to be seen, but at this juncture none of these "advected" boundaries seem to work well.

B. Advection of Moisture

We performed experiments with respect to the advection of moisture to assess the importance of this parameterization on the performance of the model. In general, the differences in advection schemes did not translate into major differences in the other variables. There were, however, substantial differences in the moisture distribution and even more in the predicted precipitation. As we continued our experiments, we found that many other modifications seemed to have a major impact on the precipitation. All indications were that the convective schemes, both the original Kuo and the modified Kuo, are very sensitive to moisture distribution and especially moisture convergence. With slight changes in the numerics, large differences in precipitation amounts seem to occur.

As mentioned in the introduction, we were forced to recast the physical parameterizations (i.e., the PBL and moist processes) in the solution sequence as adjustments to forecast values rather than adjustments to tendencies, in order to accommodate the Lagrangian advection. The Eulerian advection that was performed originally, resulted in large amounts of precipitation whereas when the physics was placed after the forecast values had been updated, the Eulerian advection produced much less precipitation. This change will be demonstrated later in discussing the physical parameterizations.

Figs. 6a - 6c show the forecast 12 h accumulation of precipitation by the GSM, RLAM with (the original) Eulerian advection, and RLAM with Lagrangian advection, respectively. Verification statistics are not readily available, but the National Weather Service (NWS) weekly summary shows 24 h accumulated maximum of 1.1 in (2.8 cm) around the Washington, D.C., northern Virginia area. The nearly 3.8 cm maximum for 12 h in 6b thus seems excessive for this storm. Figs. 7a - c depict the 48 h forecast specific humidity distribution at 850 mb for the same models in Fig 6. Fig 7d is the FGGE IIIB analysis valid at the same time. All models correctly (at least qualitatively) predict the dry interior of the U.S. and the moist surge on the East Coast. The extent of the northward advance of large amounts of moisture on the East Coast is mostly misforecast especially by RLAM due mostly to the underestimation of the intensity of the Presidents' Day storm as we mentioned in our last report (Gerlach, 1988). All models also overdo the drying in the eastern North Atlantic, again due probably to a poor synoptic forecast in that region. What is more noteworthy is the similarity between the Eulerian and Lagrangian forecasts, despite the discrepancy in precipitation amounts which should have had some feedback on other variables. True, the

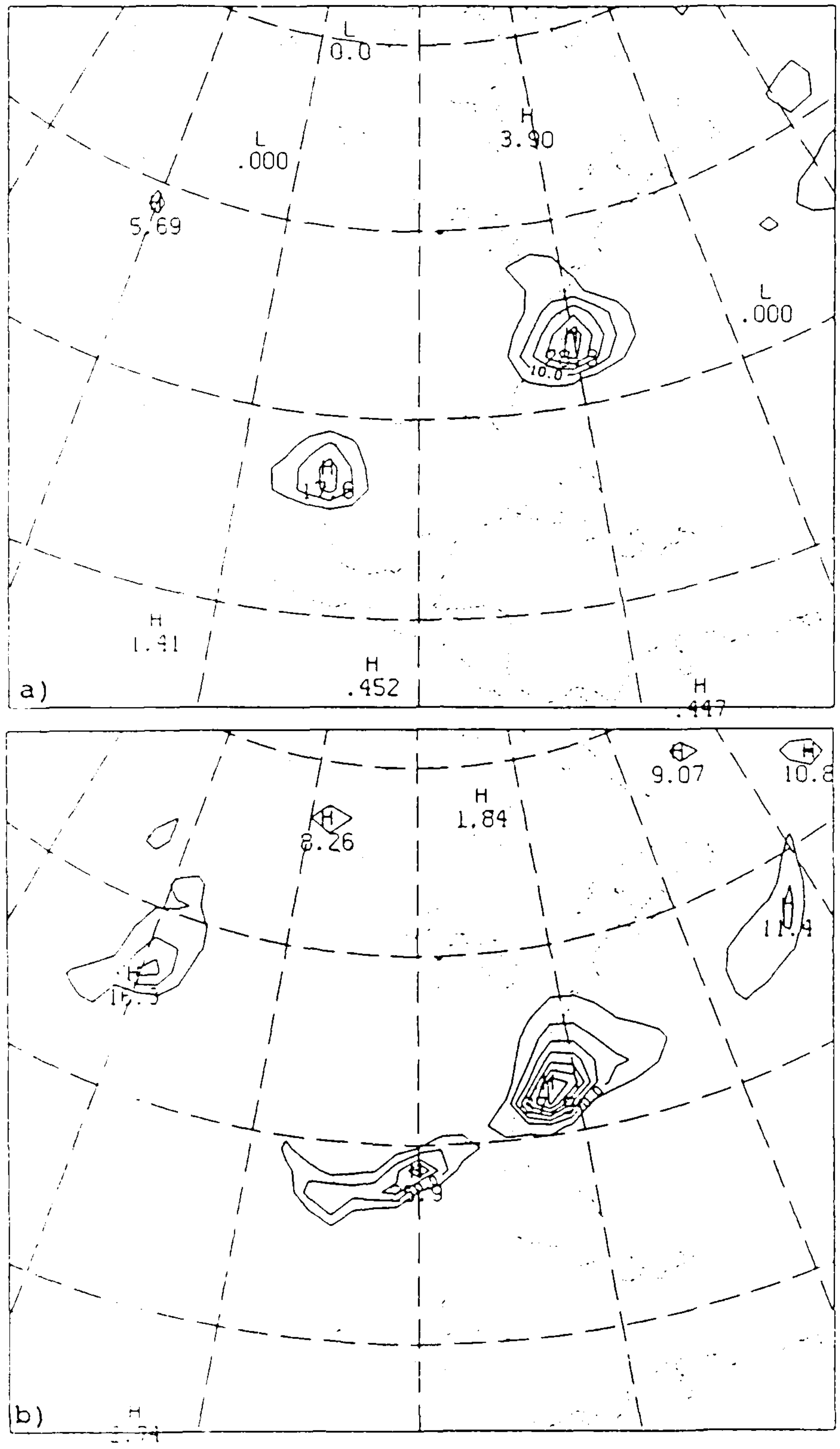

Figure 6

12 h accumulated precipitation (mm) from a 48 h forecast valid at 1200 UTC 19 February 1979 produced by a) GSM, b) RLAM with Eulerian advection of moisture, update performed on the tendencies, and c) RLAM with Lagrangian advection of moisture.

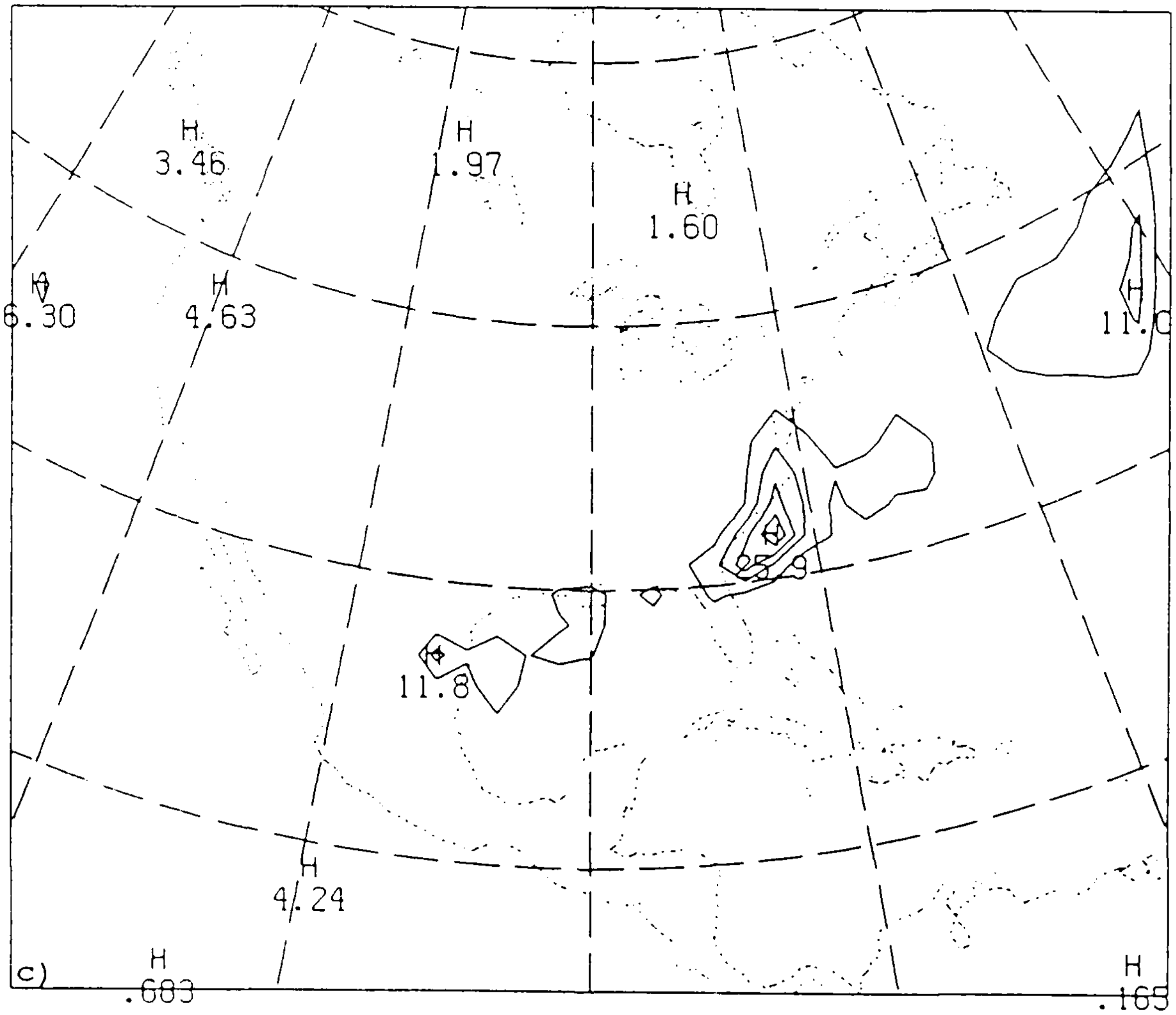
H
3.46
H
1.97
H
1.60
H
6.30
H
4.63
H
11.8
H
4.24
c)
H
.683
H
.165

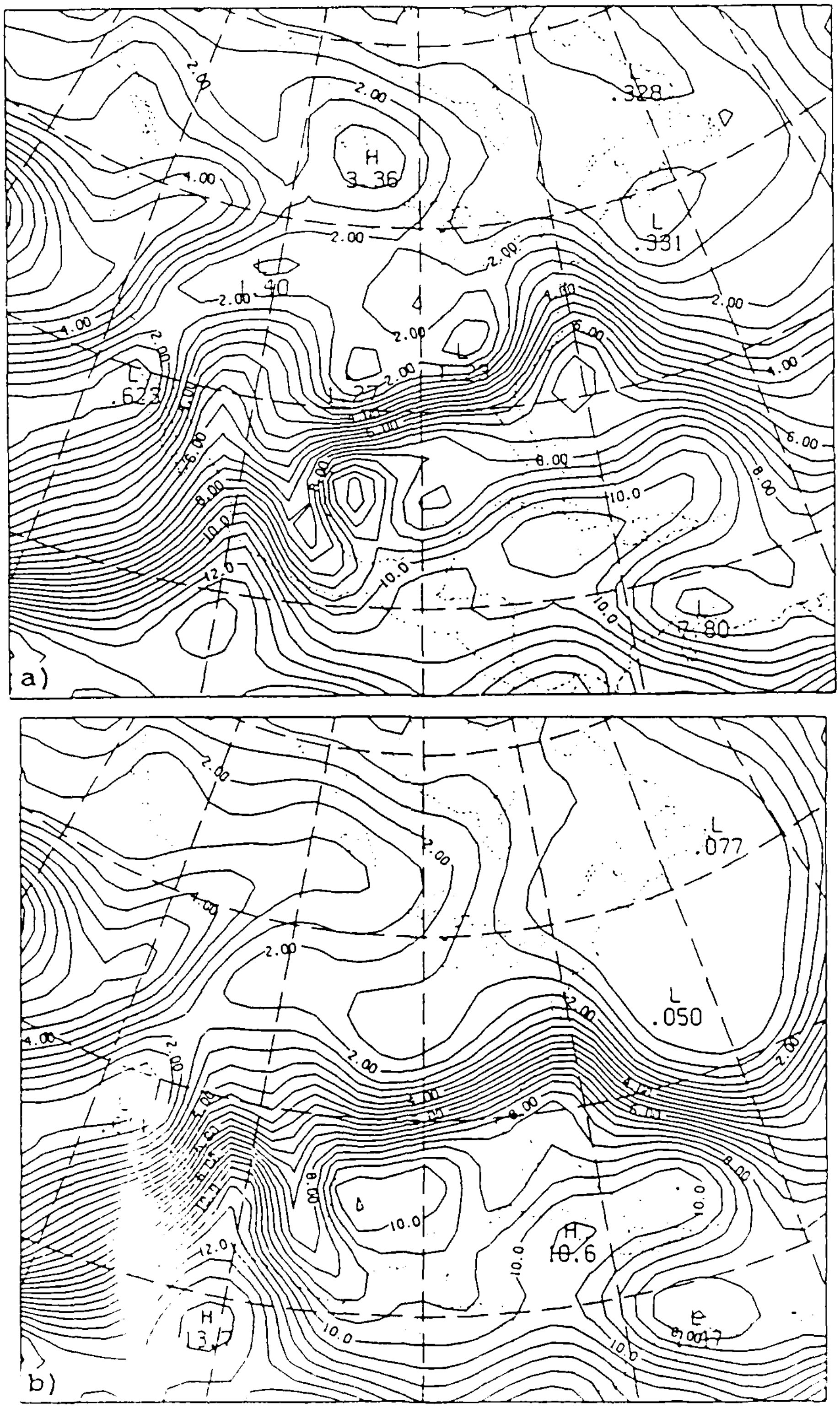

Figure 7

Forecast 48 h specific humidity (gm kg^{-1}) at same time and by same models as Fig. 6 plus d) FGGE IIIB analysis of specific humidity at same time.

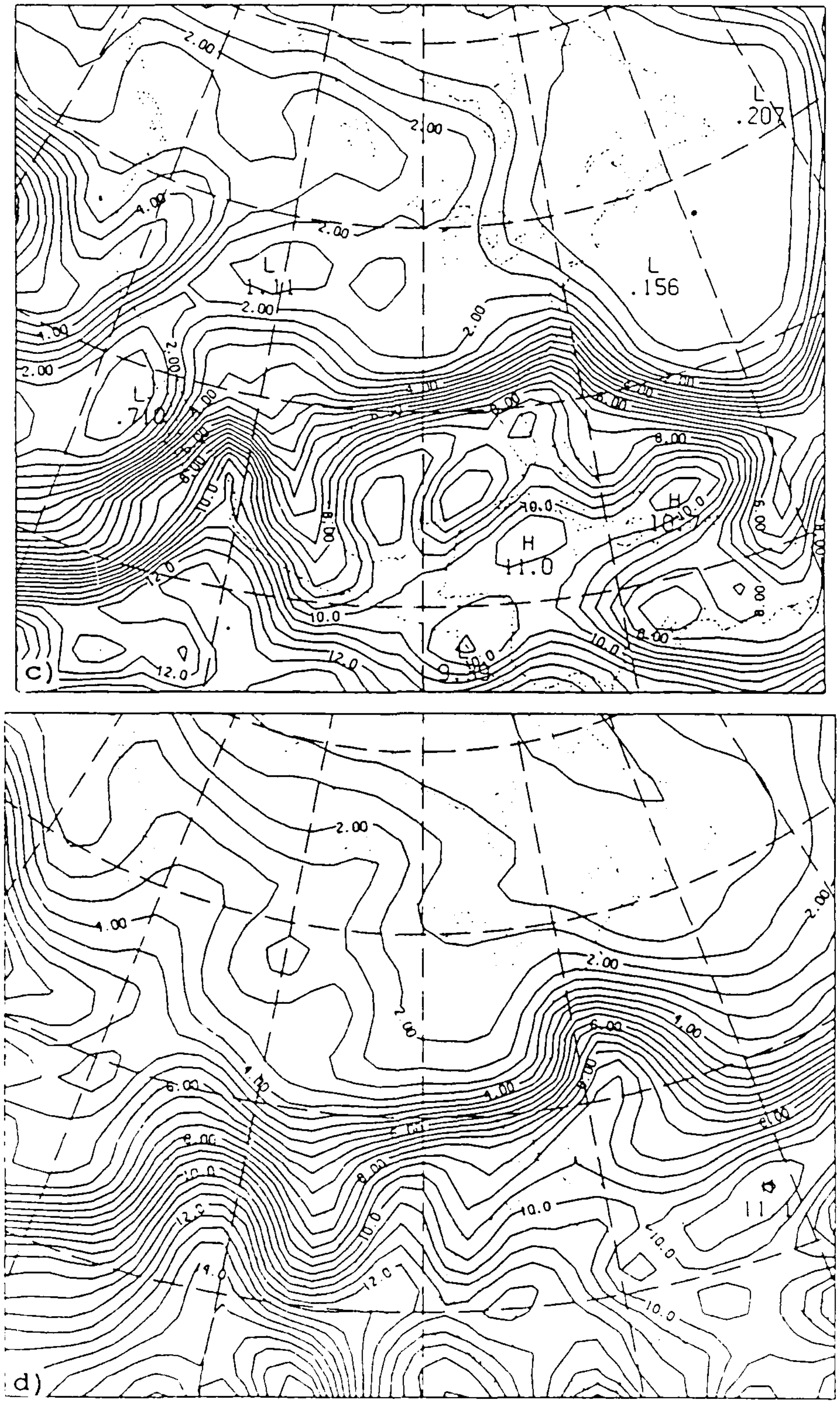

2.00
L
.207
4.00
L
1.14
L
.156
L
.710
8.00
10.0
H
11.0
12.0
9.39
c)
6.00
d)

Lagrangian scheme does appear a bit moister for not having lost as much in precipitation, but the two schemes result in very much the same forecast. The boundaries are an exception but that is due to an error in programming that failed to update the boundaries at each time step, which was corrected only a short while before the end of the project. After correction, the boundaries resemble the Eulerian boundaries. We checked the interior and found that it did not change much after the correction, probably because the Lagrangian scheme uses the boundaries only as a new source of moisture. The advection process is slow and will normally not move moisture too far in 48 h especially at lower levels where average wind speeds are of the order of 10 ms^{-1}. Further and more extensive testing of Lagrangian and Eulerian advection was performed in concert with the new physical parameterizations and will be discussed in the next section.

C. Physics

Changing the physical parameterizations on RLAM and GSM had a far reaching effect on model forecasts. One beneficial outcome of the new PBL and modified Kuo (Mod Kuo) scheme was a superior GSM Presidents' Day forecast. As we reported in our previous study (Gerlach, 1988) the GSM actually performed worse with regard to this storm when the vertical resolution was increased from 12 to 17 layers. Yet, with neither resolution was the storm fully developed. RLAM fared no better, no matter which numerical device was turned on, except in contrast to the GSM, an increase of vertical resolution led to a slightly better forecast. Fig. 2 is the FGGE IIIB analysis at 1200 UTC 19 February 1979, Fig. 8a is the GSM 48 h forecast valid at the same time, produced with the older version of the physics, and Fig. 8b is the GSM 48 h forecast produced with Mod Kuo and the OSU PBL. Table I emphasizes the improvement by comparing the root mean squared (RMS) differences and the mean differences between the models and the analysis of temperature at 12 mandatory levels and sea level pressure. (The FGGE IIIB data actually underwent a double interpolation: from FGEE to sigma layers then back to mandatory.) There is a dramatic lowering of both the root mean-square error and mean error (bias) throughout the atmosphere with the introduction of the new physical packages.

RLAM forecasts did not fare as successfully in this case. In fact, they appeared quite similar to the forecasts already discussed in Gerlach (19 8). (For the other two scenarios, we did not run the GSM with the new physics but, as we already mentioned, those presented no major forecasting problem even with the old physics.) Table II shows the RMS errors and biases of various RLAM forecasts. For all RLAM forecasts, vertical resolution was 17 layers for the old PBL and 18 layers for the OSU PBL. Horizontal resolution was one-half standard mesh for the North American cases and one-third mesh for the European case, unless otherwise stated. The time steps were 180 s for North America and 120 s for Europe. In terms of rms errors, the very highest layers with the OSU PBL tend to be a little high. What is interesting, though, is the

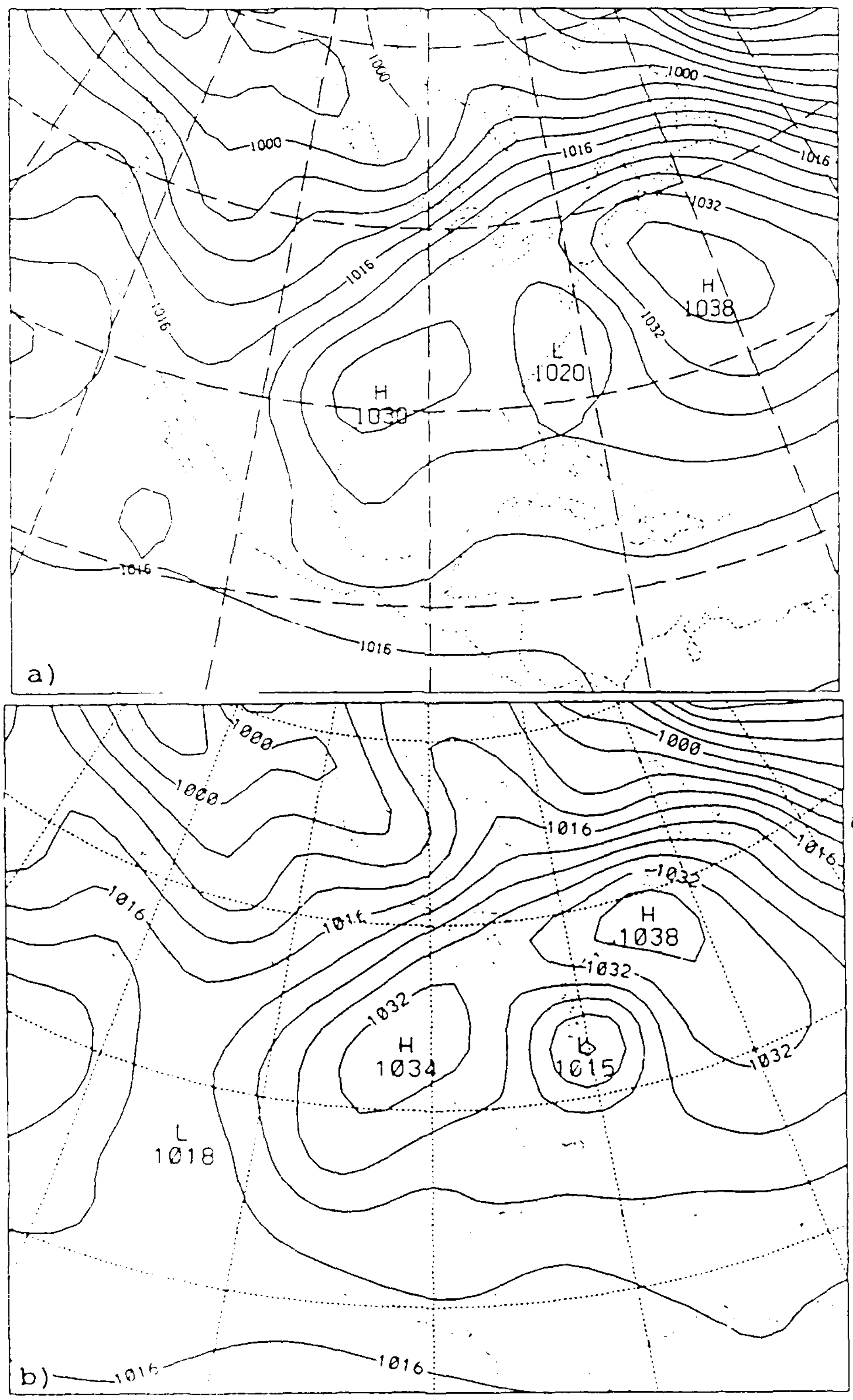

Figure 8

GSM 48 h forecast of sea-level pressure valid at 1200 UTC 19 February 1979 with a) 17 layers and old physics and b) 18 layers, OSU PBL, and Mod Kuo.

TABLE I

RMS (and mean) differences between FGGE IIIB analysis and GSM 48 h forecasts (analysis-forecast) made with new and old physics parameterizations for 1200 UTC 19 February 1979.

		Temperature (°C)		Surface Pressure (mb)	
Level	mb	New	Old	New	Old
1	1000	4.66 (0.19)	6.89 (2.20)	4.29 (1.65)	6.53 (4.35)
2	850	2.67 (0.93)	2.41 (-.036)		
3	700	1.85 (0.49)	2.19 (-1.04)		
4	500	1.69 (0.46)	2.12 (-1.26)		
5	400	1.61 (0.20)	2.01 (-1.20)		
6	300	1.45 (-0.006)	1.86 (-1.20)		
7	250	1.72 (-0.56)	1.81 (-0.84)		
8	200	2.12 (-0.85)	1.82 (-0.38)		
9	150	1.73 (-0.26)	1.57 (-.029)		
10	100	1.45 (-0.18)	2.13 (1.38)		
11	70	1.88 (-0.30)	2.08 (1.10)		
12	50	1.62 (-0.16)	2.39 (-.44)		

TABLE II

RMS (and mean) differences between FGGE IIIB analysis and RLAM 48 h forecast with Mod Kuo, OSU PBL, and Mod Kuo plus OSU PBL verifying at 1200 UTC 19 February 1979 for temperature and surface pressure.

		Temperature (°C)			Surface Pressure (mb)		
Level	mb	Mod Kuo	OSU PBL	Mk + PBL	Mod Kuo	OSU PBL	MK + PBL
1	1000	7.91 (-2.16)	7.92 (3.17)	7.71 (2.95)	6.72 (-3.94)	6.32 (0.49)	6.03 (-0.94)
2	890	2.55 (-0.23)	3.91 (0.79)	3.61 (0.25)			
3	700	1.93 (0.65)	2.20 (0.64)	2.09 (-0.28)			
4	500	1.91 (0.97)	1.95 (0.77)	1.81 (-0.14)			
5	400	1.92 (1.05)	2.01 (0.58)	1.79 (-0.14)			
6	300	1.82 (1.15)	1.83 (0.84)	1.69 (0.43)			
7	250	1.73 (0.78)	1.73 (0.63)	1.82 (0.68)			
8	200	1.72 (0.38)	1.78 (0.27)	2.03 (0.62)			
9	150	1.54 (0.07)	1.55 (-0.02)	1.60 (0.03)			
10	100	2.09 (-1.31)	1.59 (-0.82)	1.47 (-0.04)			
11	70	2.00 (-1.04)	3.07 (-1.84)	1.87 (0.08)			
12	50	2.35 (0.36)	2.93 (-1.73)	1.64 (0.03)			

large bias at the lowest layer. Here the old physics on the GSM and the OSU PBL with the old Kuo scheme have a large positive bias, i.e., the model is too cold at the lowest two levels. Mod Kuo, on the other hand, has a negative bias indicating the lower layer is too warm. When the PBL is combined with Mod Kuo, the bias is reduced along with the rms error. For the GSM the combination works very well; the two processes complement each other and produce a good forecast. With RLAM, the combination does not work as well. A substantial cold bias remains and the storm does not develop to its expected intensity.

For the case of the January storm, the situation is a bit different. Fig. 3 shows the sea level pressure contours valid at 0000 UTC 25 January 1979 over North America. At this point an intense well-occluded storm is seen entrenched over Pennsylvania, New York, and eastern Ohio with a good fetch of moist Atlantic air over most of the mid- and North Atlantic coast. Most models had little difficulty forecasting this feature but some were amiss in finding the correct position and some were incorrect in forecasting the lows in the west and the high over the Gulf. Table III shows the RMS and mean differences between the FGGE IIIB analysis and forecasts made by the GSM and RLAM with different physical parameterizations.

As already noted, only the old physics version of the GSM was available. This meant that the lateral boundary conditions for RLAM also reflected this older version. For the requirements of

TABLE III

RMS (and mean) differences between FGGE IIIB analysis and 36 h forecasts of the GSM (old physics), RLAM with Mod Kuo, RLAM with OSU PBL, and RLAM with Mod Kuo and OSU PBL for temperatures and surface pressure at 0000 UTC 25 January 1979.

Temperature (°C)

Level	mb	GSM	Mod Kuo	PBL	Mod Kuo + PBL
1	1000	5.08 (1.13)	5.93 (0.93)	6.20 (-2.58)	6.13 (-2.60)
2	850	2.31 (0.02)	2.63 (0.17)	3.15 (-0.89)	3.09 (-0.97)
3	700	1.82 (-0.77)	1.84 (-0.23)	1.96 (-0.33)	1.97 (-0.27)
4	500	2.10 (-0.93)	1.98 (0.18)	2.06 (-0.27)	2.01 (-0.23)
5	400	2.06 (-0.93)	2.01 (-0.29)	2.11 (-0.15)	2.04 (-0.21)
6	300	1.65 (-0.69)	1.76 (-0.35)	1.73 (-0.11)	1.80 (-0.20)
7	250	1.84 (-0.39)	1.96 (-0.37)	1.93 (-0.13)	2.00 (-0.23)
8	200	1.89 (0.08)	2.00 (-0.24)	2.01 (-0.07)	2.02 (-0.14)
9	150	1.60 (0.07)	1.62 (-0.06)	1.70 (0.00)	1.64 (0.01)
10	100	1.89 (0.49)	1.69 (0.47)	1.62 (0.17)	1.60 (0.21)
11	70	1.93 (0.66)	1.72 (0.25)	2.70 (1.10)	2.72 (1.14)
12	50	2.35 (0.67)	2.27 (0.47)	3.40 (2.16)	3.44 (2.19)
Surface Pressure (mb)		3.51 (-0.77)	3.65 (-1.50)	6.17 (-4.91)	6.07 (-4.84)

the OSU PBL, it was also necessary to interpolate from the 17-layer version of the GSM to an 18-layer structure which added more resolution in the boundary layer. Also in the verification data in Table III some of the files were interpolated from 17 to 12 layers (FGGE IIIB, GSM, and RLAM with Mod Kuo), while the OSU PBL forecasts were interpolated from 18 to 12 layers. Part of the errors in the lowest and highest layers are no doubt attributable to the cumulative interpolation errors (including the interpolation at the boundaries and for the verification). Evidence of this was found when we compared initial fields, and, when we repeated the Mod Kuo experiment with 18 instead of 17 layers, the RMS errors appeared much closer to the Mod Kuo + PBL errors of Table III. In fact the lowest layer temperature RMS was over 7°C. The biases, however, were not as pronounced nor necessarily of the same sign as the PBL experiments. The biases with the PBL here are, in contrast with the Presidents' Day case, negative in the lowest layers indicating a warming in the boundary layer. At uppermost levels the bias is positive indicating a commensurate cooling in the stratosphere.

RMS differences and biases in Table IV for the third scenario involving the North Sea in summer shows very little difference between models. Here again the GSM has the older physics whereas RLAM with the PBL was run with 18 layers and the lateral boundary data were interpolated from the 17-layer GSM forecast. Most of the mid-level errors are due to a bias (mostly an overestimate of temperature) which turns around at the topmost levels. The surface

TABLE IV

RMS (and mean) differences between FGGE IIIB analysis and 48 h forecasts of temperature and surface pressure by GSM (old physics), RLAM with Mod Kuo, RLAM with Mod Kuo and OSU PBL, and RLAM with Mod Kuo and OSU PBL with fourth order differencing for 1200 UTC 26 June 1979 over Europe and the North Sea.

Temperature (°C)

Level	mb	GSM	Mod Kuo	Mod Kuo + PBL	MK + PBL (4th order)
1	1000	5.95 (0.51)	5.79 (0.75)	5.54 (1.07)	5.59 (1.10)
2	850	2.91 (-0.23)	2.88 (-0.08)	3.02 (0.03)	3.07 (0.17)
3	750	1.91 (-0.99)	1.88 (-0.99)	1.67 (-0.55)	1.59 (-0.37)
4	500	1.78 (-0.84)	1.77 (-1.10)	1.81 (-0.48)	1.88 (-0.47)
5	400	1.97 (-1.04)	1.93 (-1.31)	1.90 (-0.73)	2.01 (-0.79)
6	300	1.94 (-1.11)	2.10 (1.48)	2.15 (-1.43)	2.24 (-1.54)
7	250	1.97 (-0.89)	1.99 (-1.12)	2.23 (-1.44)	2.25 (-1.45)
8	250	1.78 (-0.80)	1.64 (-0.68)	1.85 (-0.95)	2.00 (-0.95)
9	150	1.41 (-0.37)	1.34 (-0.20)	1.39 (-0.33)	1.50 (-0.44)
10	100	0.94 (0.42)	1.04 (0.61)	1.01 (0.34)	0.98 (0.15)
11	70	1.08 (0.47)	1.31 (0.88)	1.29 (0.91)	1.19 (0.66)
12	50	1.08 (0.30)	1.26 (0.75)	1.77 (1.53)	1.58 (1.29)
Surface Pressure (mb)		3.28 (2.34)	3.31 (0.56)	5.03 (-3.45)	4.90 (-2.51)

pressure errors are more pronounced with the PBL but this could be a result of the interpolation near the surface. We tried to see what effect a change to fourth order differencing would have on the results. As one can plainly see the impact is secondary to the effects of the physics. We found the same to be true when we ran the January case with fourth order differencing. The supposed reduction of truncation error due to higher order differencing is not noticeable in these forecasts, neither objectively through RMS error analyses nor through subjective map evaluation. We also repeated the Presidents' Day forecast by including the OSU PBL and Mod Kuo and doubling the horizontal resolution. As can be imagined, this greatly increased the execution time of the model, so that we performed only one high-resolution experiment. As opposed to previous high-resolution experiments, reported by Gerlach (1986), where a doubling of resolution was coupled with a halving of the domain size, this experiment maintained the original domain size to avoid complications with closer lateral boundaries.

Figs. 9a and 9b show the high resolution 48 h forecast of 500 mb heights and sea level pressure, respectively, valid at the same time as Fig. 2. The Presidents' Day storm was forecast inland rather than at the coast. The 500 mb heights do exhibit more of a trough than lower resolution forecasts, but it is placed a little too far west. Thus, higher resolution, while undoubtedly affecting the forecast, does not necessarily make it better. In fact, the successful Presidents' Day forecast of the GSM was made with a relatively low resolution of 30 rhomboidal waves. Attempts to

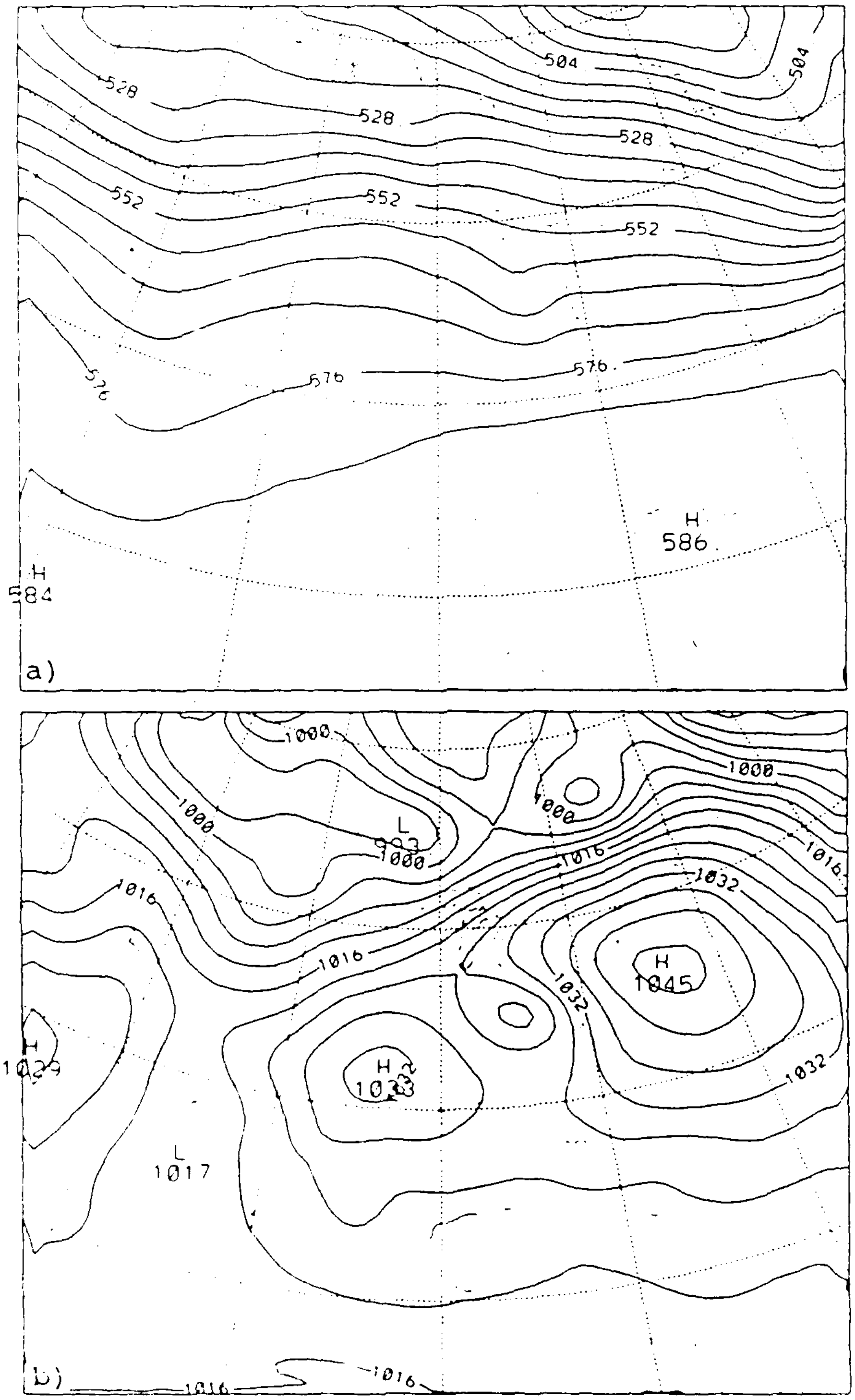

Figure 9

RLAM high resolution (1/4 mesh) with OSU PBL and Mod Kuo 48 h forecast of a) 500 mb heights and b) sea-level pressure valid at 1200 UTC 19 February 1979.

forecast the storm with the latest Relocatable Window Model (RWM) of Global Weather Central (GWC) was equally unsuccessful. This leads us to the conclusion that for this specific case, limited-area models are no better than global spectral models despite their higher resolution. It would be very tempting to discover why this is so.

D. Moisture Considerations

One of the major considerations in experimenting with numerical and physical parameterizations is to ascertain which combinations can lead to better moisture forecasts. A major problem in assessing a moisture forecast is the lack of dependable verification. Even in areas where dense networks of observations exist, the analysis of humidity is probably poor to fair due to large observation errors, especially in the upper atmosphere, and poor sampling of water vapor which, as is well known, does not vary smoothly in space. Cloud pictures can help in determining areal coverage but are almost useless in delineating vertical distribution. Precipitation measurements are also fraught with error because of non-representative samplings in isolated populated locations as well as different conventions regarding frequency of accumulation measurements. Our comparisons, then, become more qualitative than quantitative. In areas over North America where the NMC Weekly Summary depicts 24 h accumulation, we can do some graphic comparison of amounts. For humidity, we will rely on FGGE IIIB analyses for verification.

Fig. 10a is the FGGE IIIB analysis of moisture at 850 mb at 0000 UTC 25 January 1979. Fig. 10b is the 24 h accumulated precipitation valid the next morning at 1200 UTC 25 January 1979 as portrayed by the NWS Weekly Summary. Unfortunately, the precipitation contours from NWS do not extend over the ocean, where a great deal of activity must have taken place. Fig. 11a shows 12 h accumulations for a 36 h forecast predicted by RLAM valid at 0000 UTC 25 January with the original (tendency modified) Eulerian advection of moisture with the Mod Kuo scheme but with the old boundary layer parameterization (17-layers, as well). Fig. 11b is the same as Fig. 11a but where the updates are performed after the forecast. Fig. 11c is the same as Fig. 11b, except that the forecast was performed with an 18-layer RLAM, with initial and boundary data interpolated to 18 layers from 17 layers. Fig. 11d is the same as Fig 11c with the old Kuo scheme and the OSU PBL parameterization and Fig. 11e has both Mod Kuo and OSU PBL. In comparison Fig. 11f is the result of Mod Kuo with the old PBL and Lagrangian advection of moisture. It is interesting to note at this point that the largest differences in forecast amounts are due to the position of the physical parameterization in the sequence of the model, i.e., whether the physics affects the tendencies or the variables themselves. Otherwise, there are distinguishable effects in the amount and location of precipitation as one adds or subtracts physical parameterizations. The Mod Kuo run of Fig. 11b shows very little precipitation and most of it probably too far north and inland. The change in layering helps a little and gives a more realistic precipitation pattern. The OSU PBL with or

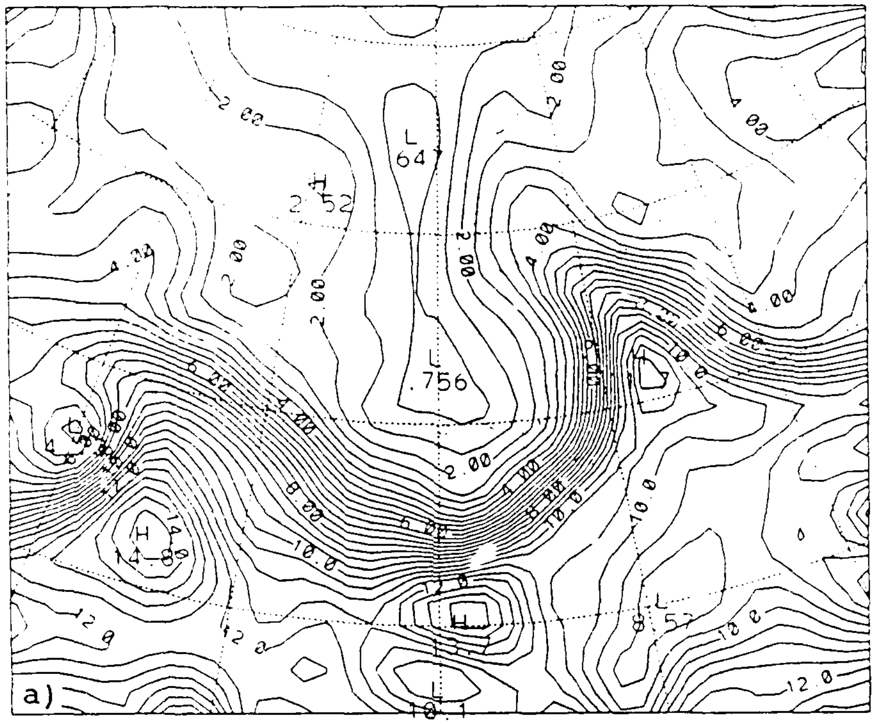

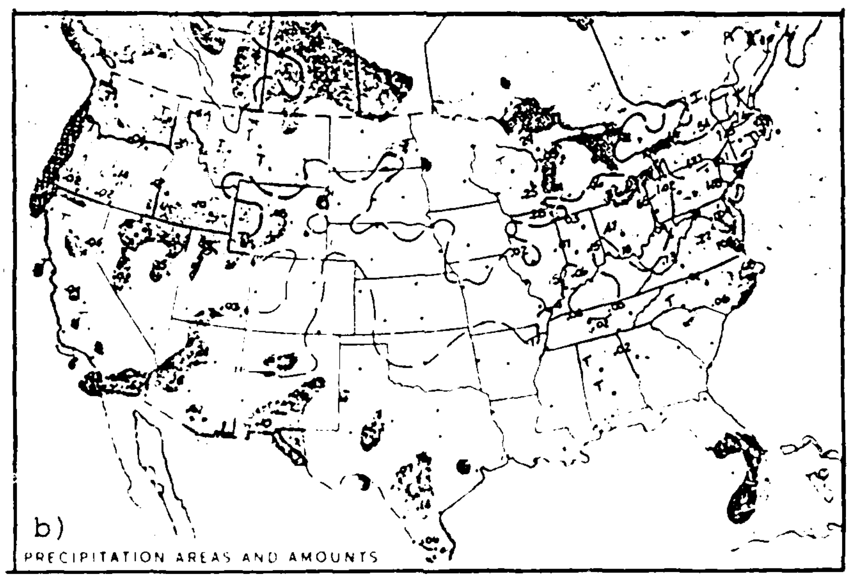

Figure 10

a) FGGE IIIB analysis of specific humidity (gm kg^{-1}) at 850 mb for 0000 UTC 25 January 1979. b) NWS analysis of 24 h accumulated precipitation (inches) valid at 1200 UTC 25 January 1979.

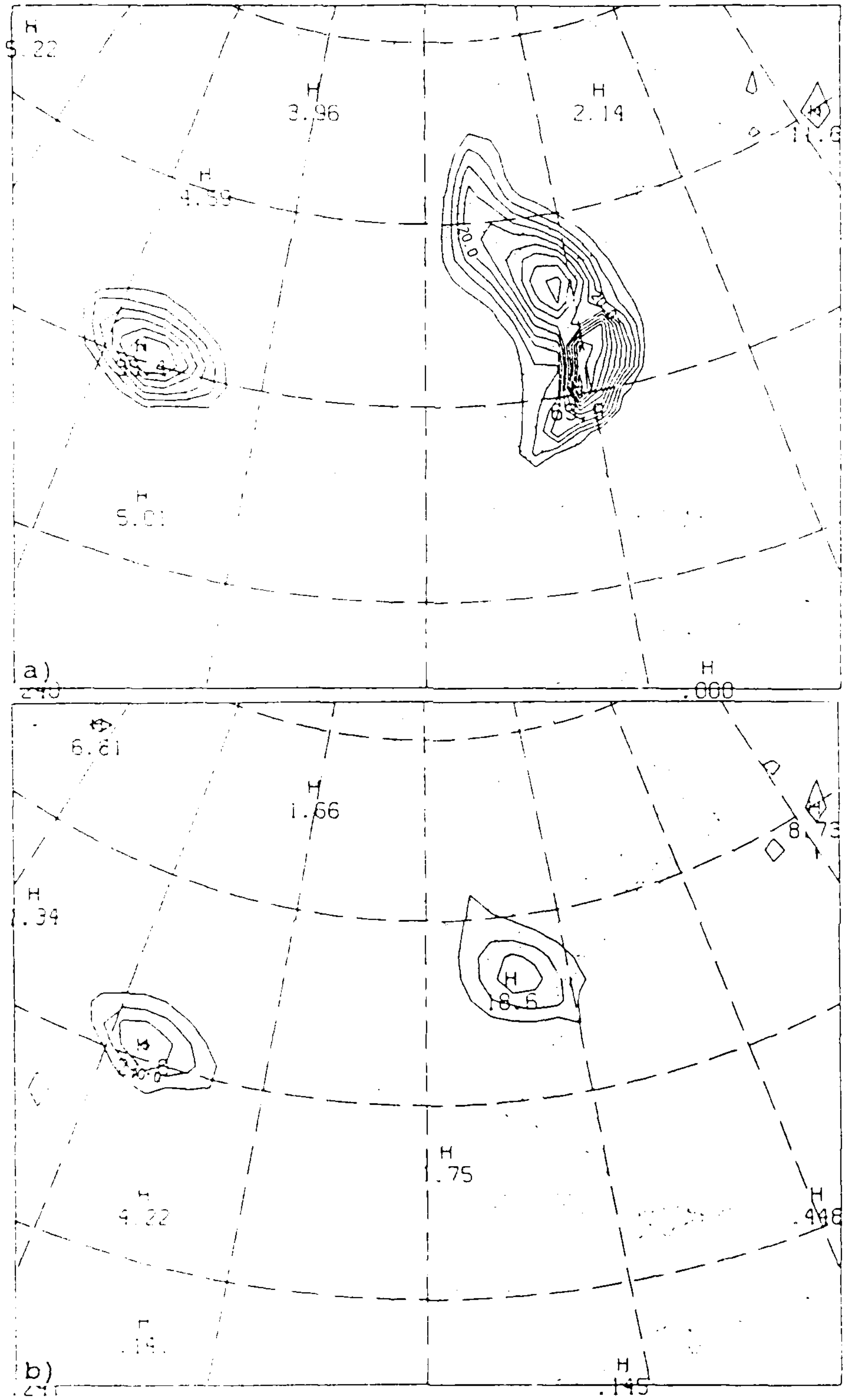

Figure 11

36 h forecast of 12 h accumulated precipitation (mm) valid at 0000 UTC 25 January 1979 by RLAM with a) Eulerian advection of moisture (tendency update), Mod Kuo, and old PBL; b) same as a) but with variable updates; c) same as b) but with interpolation to 18 layers; d) Eulerian advection (variable update), old Kuo, and OSU PBL (18 layers), e) Eulerian advection (variable update), Mod Kuo, and OSU PBL, and f) Lagrangian advection, old PBL (17 layers), and Mod Kuo.

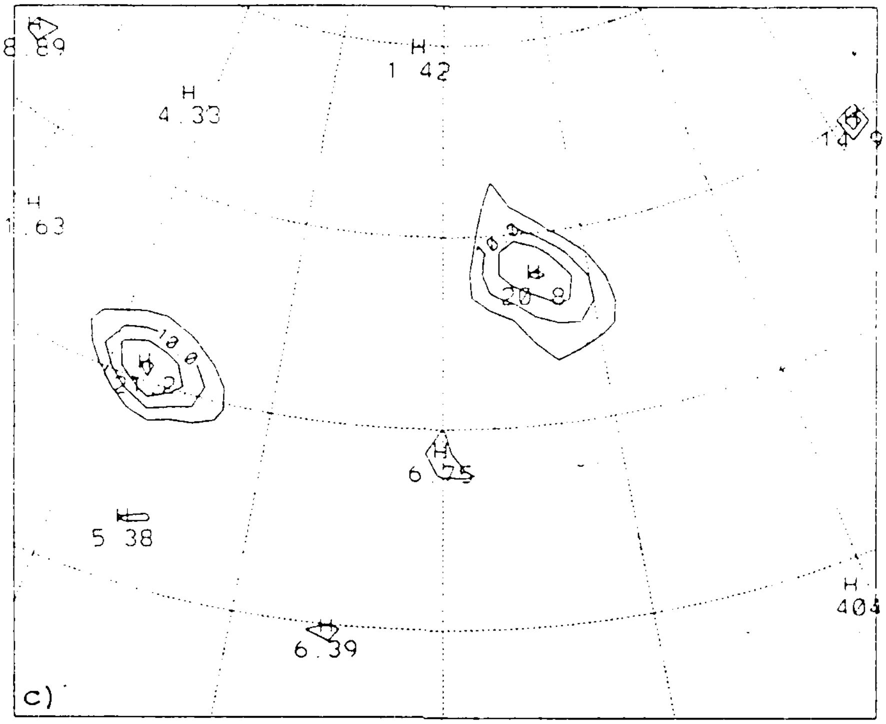
c)

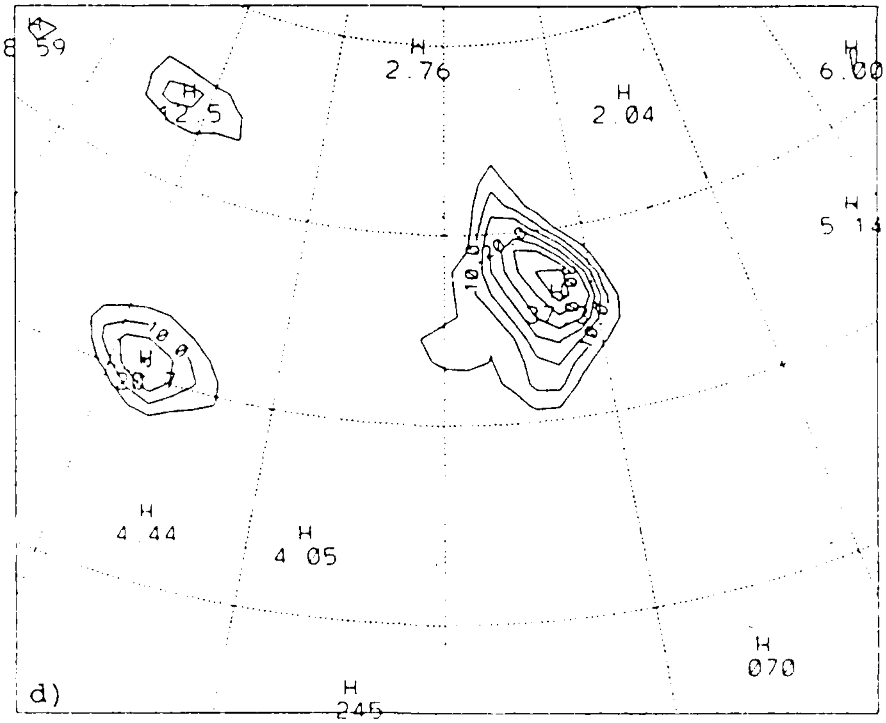
d)

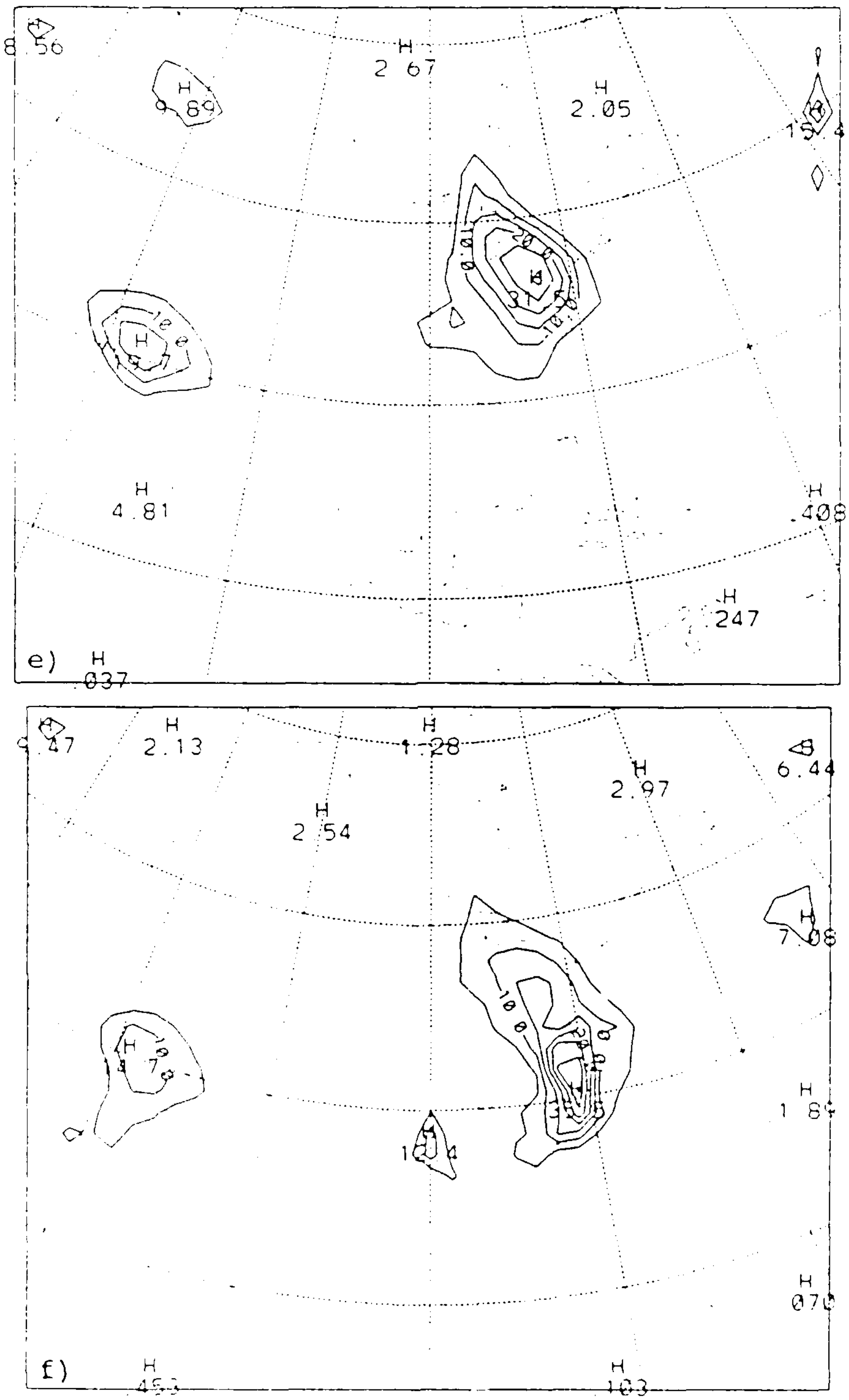
H
2.67
H
2.05
H
9.89
H
4.81
H
.408
H
.247
e)
H
.037
H
2.13
H
1.28
H
2.97
6.44
H
2.54
H
7.08
H
1.89
H
.070
f)
H
.453
H
.103

without Mod Kuo results in greater amounts, but the maximum still is predicted north and west of where it actually occurred. Lagrangian advection with Mod Kuo with the old PBL provides about the same amount of precipitation as the Eulerian schemes with the OSU PBL, but far to the south and east of them.

Tables V and VI give the RMS differences and biases in specific humidity for the various models. It is clear that the most significant impact is delivered by the OSU PBL which tends to dry the lower atmosphere and severely moisten the upper atmosphere. The percentage RMS errors at the lowest levels for all models are substantial, indicating the difficulty in forecasting moisture with any model. The models with the old PBL tend to have the same magnitude and sign of RMS errors and biases, especially at higher levels. The latter Eulerian scheme that updates the variables instead of tendencies keeps the lowest layers abnormally dry while lowering the precipitation amount. The dryness is not compensated by moistening of the upper atmosphere, begging the question as to where the moisture has gone. The OSU PBL, on the other hand, increases precipitation while moistening the upper levels of the atmosphere substantially, leading to the complementary question as to where the excess moisture is coming from. One would be inclined to say that in the case of the OSU PBL the moisture flux from the surface is enhanced by the new physical parameterization, but lacking a clear moisture budget calculation at this point renders this explanation mere speculation. In comparing Lagrangian vis-a-vis Eulerian advection i.e., Table V,3 compared with VI,2 and V,4

TABLE V

RMS (and mean) differences between FGGE IIIB and 1. GSM with original physics, 2. RLAM Eulerian advection with Mod Kuo and old PBL and modified tendencies, 3. RLAM Eulerian advection with Mod Kuo and old PBL with updated variables, 4. RLAM Eulerian advection with old Kuo and OSU PBL, and 5. RLAM with Eulerian advection Mod Kuo and OSU PBL, for 36 h forecasts of specific humidity (g kg^{-1}) valid at 0000 UTC 25 June 1979 over North America.

Level	mb	1.	2.	3.
1	1000	2.06 (0.32)	2.61 (0.53)	3.73 (1.90)
2	850	2.12 (0.33)	2.22 (0.51)	3.46 (1.93)
3	700	1.18 (-0.08)	1.15 (0.01)	1.54 (0.64)
4	500	0.56 (-0.04)	0.55 (-0.08)	0.60 (0.10)
5	400	0.34 (-0.03)	0.35 (-0.09)	0.32 (-0.00)
6	300	0.25 (-0.04)	0.28 (-0.11)	0.24 (-0.06)

Level	mb	4.	5.
1	1000	1.96 (0.06)	2.01 (0.16)
2	850	2.68 (0.74)	3.11 (1.07)
3	700	1.57 (0.46)	1.57 (0.48)
4	500	1.83 (-1.05)	1.82 (-1.06)
5	400	2.25 (-1.66)	2.25 (-1.67)
6	300	2.51 (-1.98)	2.51 (-1.99)

TABLE VI

Same as Table V except for FGGE IIIB versus 1. Eulerian advection with Mod Kuo, OSU PBL, and fourth order differencing, 2. Lagrangian advection with Mod Kuo and old PBL, 3. Lagrangian advection with old Kuo and OSU PBL.

Level	mb	1.	2.	3.
1	1000	2.98 (1.08)	2.90 (0.52)	1.86 (-0.98)
2	850	3.93 (1.98)	2.35 (0.60)	2.20 (-0.24)
3	700	1.67 (0.84)	1.33 (0.03)	1.46 (-0.17)
4	500	1.44 (-0.71)	0.63 (-0.06)	2.44 (-1.71)
5	400	1.84 (-1.32)	0.40 (-0.06)	2.98 (-2.32)
6	300	2.10 (-1.64)	0.32 (-0.08)	3.27 (-2.64)

compared with VI,3, it is clear that Lagrangian advection tends to keep the atmosphere moister at all levels. In this case this happens to reduce the RMS error in the lower levels, but increases it in the upper atmosphere. The total precipitation amounts (not shown) are about the same for both advections when the OSU PBL is used, but the Lagrangian advection produces more precipitation than Eulerian advection (updating the variable) with the old PBL. The results from the summer case over the North Sea are about the same, namely, the OSU PBL tends to moisten the upper atmosphere too much, while the Lagrangian advection results in a slightly moister atmosphere throughout.

IV. Summary and Conclusions

A series of experiments was performed with various physical and numerical parameterizations to test which combinations would work best in the context of RLAM especially with regard to moisture prediction. Our first experiments involved various types of lateral boundary specifications. They were from the class of "radiation" boundaries first proposed by Orlanski (1976), where the phase speed of a variable is allowed to advect the variable out of the domain if that is the direction of motion or to substitute the externally provided values if the direction is inwards. One could treat each variable separately or one could use an average velocity to advect all variables. A similar approach was taken where Lagrangian advection of boundary points were substituted for the phase speed advection of the radiation boundary. Here, the advected points act as sources for an interpolation or extrapolation to the boundary. One can select how many points should be involved in the analysis of the boundary. These experiments showed that all these boundary treatments are not dependable and require a great deal more investigation and "tweaking" before any can be put to practical use. The Lagrangian advected boundaries, for example, ranged between having no effect (i.e., no better than if the external boundary specified the outer row at each time step) to creating a very noisy and nearly unstable forecast, with the many optional parameters being the determinant of the outcome.

Physical parameterizations involving the convective and planetary boundary layer processes were studied. The original parameterizations were taken from NMC's QNGM (Mathur, 1983) and consisted of a Kuo convective scheme and a bulk parameterization of boundary processes. A modified Kuo and sophisticated PBL parameterization were substituted for the original ones. Lagrangian and Eulerian advection schemes were also incorporated into the model. Various combinations of the physical packages were tested and verified against FGGE IIIB analyses. These experiments were inconclusive. The new physics in concert with the GSM furnished a very convincing forecast of the Presidents' Day storm. This was not duplicated with RLAM which could not, under any combination of physics or numerical devices (including a doubling of horizontal resolution), be coaxed into creating an accurate forecast of the storm. As for moisture distribution, higher vertical resolution and the OSU PBL produced more precipitation. The OSU PBL also tended to moisten the upper atmosphere too much while drying the lower atmosphere. Lagrangian advection also seems to provide more moisture throughout the atmosphere than the Eulerian schemes.

These experiments lead us to conclude that physical parameterizations cannot be tested independently of numerical devices. Certainly, model resolution is related to model performance and sometimes is dictated by the requirements of the physics, as in the case of the OSU PBL. Other physical models, such as the convective routines are also very sensitive to model numerics and algorithm. Changing from Lagrangian to Eulerian advection had a profound effect on precipitation output, as did repositioning of the convective subroutines. This implies that developers of physical parameterizations serve no purpose in testing and tuning their parameterizations apart from the models for which they are intended. Parameterizations that produce results that are close to tested observations could be woefully lacking when applied to numerical models of the atmosphere. Our recommendations based on these and other conclusions are forthcoming in the final section.

V. Recommendations

Results of the previous section are based on the limited number of experiments made for three independent scenarios. To better understand the various parameterizations and their interaction, we should do many repetitions of these experiments as finances and time permit. These should include several tropical cases as well as Southern Hemisphere events. It is quite possible that what seems to work well in our tests will not do so in other seasons or other locations, or vice versa.

To enhance the utility of RLAM, it should be optimized in terms of computational efficiency. This includes finding an appropriate numerical scheme (such as a different semi-implicit scheme) which would allow larger time steps than the present 120 - 180 s. It also means vectorizing the code so that it takes full advantage of the Cray's potential.

The radiation and advection boundaries that we tested all tended to produce spurious noise at the boundaries. This seems to be a factor of the constant switching between outward and inward flows that cause internal and external data to alternate. The Lagrangian-advected boundary has much of the same problems but more study is required of the proposed boundary treatment before any firm statement can be issued. By balancing the region of influence with the weights, one may discover a potent combination that works. This may especially be true if larger time steps are available and the advected distance is greater. Until such experiments can be undertaken and analyzed, we suggest that radiation boundaries be avoided.

The PBL and moisture parameterizations are difficult to assess. It was shown that the OSU PBL did improve a forecast of the GSM. It, however, could not duplicate that improvement in the context of RLAM. The convective schemes, both new and old, are very sensitive to slight changes in the numerical algorithm. This sensitivity is likely produced by their dependence on moisture distribution and convergence, neither of which is well analyzed or forecast. Moisture distribution is poorly represented in grid space even with a resolution of 100 km because of moisture's high variability and the difficulties in measuring it. To overcome these problems a good convective scheme should be made less sensitive to input data and the model should be improved to better forecast the distribution and convergence of moisture.

It would be best to start with a careful analysis of the moisture budget of the model, tracing the inflow and outflow at the boundaries, evaporation from the surface, and condensation and precipitation. If possible, a concomitant analysis should be prepared for the real atmosphere, but sufficient data are probably not available. In either case, an accurate forecast of cloudiness and precipitation will require numerical and physical schemes that can correctly account for the distribution of moisture on scales currently ignored by most models.

Ritchie (1985) suggests that a quasi-Lagrangian advection of moisture better represents its movement and distribution. The quasi-Lagrangian method is hampered somewhat by the need to redefine the moisture variable at grid points at every time step. This smooths out some of the smaller scale deviations that may become important in convective processes. We can suggest correcting this by investigating the possibility of completely Lagrangian advection of moisture where interpolation to grid points is not performed. Such a scheme will present problems of keeping track of the moisture and of parameterizing convection and precipitation. The effort to solve these problems, however, may well be worthwhile.

REFERENCES

Brown, H. A. and K. A. Campana, 1978: An economical time-differencing system for numerical weather prediction, Mon. Wea. Rev., 106, 1025-1036.

Carpenter, K. M., 1982: Note on the paper Radiation conditions for the lateral boundaries of limited-area numerical models, Quart. J. Roy. Meteor. Soc., 108, 717-719.

Davies, H. C., 1976: A lateral boundary formulation for multi-level prediction models. Quart. J. Roy. Meteor. Soc., 102, 405-418.

Gerlach, A. M., 1985: Objective analysis and prediction techniques, 1985. AFGL-TR-86-0002, Contract F19628-82-C-0023, SASC Technologies, Inc., ADA169746.

____________________, 1986: Objective analysis and prediction techniques - Final Report. AFGL-TR-87-0013, Contract F19628-82-C-0023, ST Systems Corp., ADA183450.

____________________, 1988: Objective Nephology. AFGL-TR-88-0109, Contract F19628-87-C-0046, ST Systems Corp., ADA200500.

Halbertstam, I. M., 1990: Semi-implicit time scheme for RLAM, AFGL-TR-89-0324. Contract F19628-88-C-0072, ST Systems Corp.

Jiamo, Teng, 1988: A split quasi-Lagrangian method for use in a regional barotropic model. Reprints Eighth Conference on Numerical Weather Prediction, American Meteor. Soc., Boston, MA, 531-537.

Kuo, H. L. 1974: Further studies of the parameterization of the influence of cumulus convection on large-scale flow. J. Atmos. Sci., 31, 1232-1240.

Mahrt L., H-L Pan, P. Ruscher, C-T Chu, 1987: Boundary layer parameterization for a global spectral model, AFGL-TR-87-0246, Contract No. F19628-84-K-0044, Oregon State University, Corvallis, OR, ADA199440.

Mathur, M. B. 1983; A quasi-Lagrangian regional model designed for operational weather prediction. Mon. Wea. Rev., 111, 2087-2098.

McGregor, J. L., L. M. Leslie, and D. J. Gauntlett, 1978: The ANMRC limited-area model: Consolidated formualtion and operational results. Mon. Wea. Rev., 106, 427-438.

Miller, M. J., and A. J. Thorpe, 1981: Radiation conditions for the lateral boundaries of limited-area numerical models, Quart. J. Roy. Meteor. Soc., 107, 615-628.

Orlanski, I., 1976: A simple boundary correlation of unbounded hyperbolic flows. J. Comp. Phys., 21, 251-269.

Perkey, D. J. and C. W. Kreitzberg, 1976: A time-dependent lateral boundary scheme for limited-area primitive equation models. Mon. Wea. Rev., 104, 744-755.

Raymond, W. H., 1988: High-order low-pass implicit tangent filters for use in finite area calculation. Mon. Wea. Rev., 116, 2132-2141.

Ritchie, H., 1985: Application of a semi-Lagrangian integration scheme to the moisture equation in a regional forecast model. Mon. Wea. Rev., 113, 424-435.

Seitter, K. L. 1987: The specification of lateral boundary conditions in three-dimensional mesoscale numerical models, AFGL-TR-87-0015, Contract No. F19628-85-K-0008, University of Lowell, Lowell, MA, ADA179185.

Sela, J., 1980: Spectral modeling at the National Meteorological Center, Mon. Wea. Rev., 108, 1279-1292.

Shapiro, R., 1970: Smoothing, filtering, and boundary effects. Rev. Geophys. Space Phys., 8, 359-387.

Soong, S-T, Y. Ogura, W-S Kau, 1985: A study of cumulus parameterization in a global circulation model, AFGL-TR-85-0160, Contract No. F19628-82-K-0030, University of Illinois, Urbana, IL, ADA170137.

Tung, S-L, I. Halberstam, and C. Johnson, 1987: Development of an improved modular relocatable limited area model (RLAM), short- and medium-range numerical weather prediction, Special Volume of J. Meteor. Soc. Japan, T. Matsuno, ed., 485-494.